 CMES, vol.3, no.2, pp.147-173, 2002

The Emerging Role of Multiscale Modeling in Nano- and Micro-mechanics of Materials

Nasr M. Ghoniem[1] **and Kyeongjae Cho**[2]

Abstract: As a result of surging interest in finding fundamental descriptions for the strength and failure properties of materials, and the exciting prospects of designing materials from their atomic level, an international symposium on *Multiscale Modeling* was convened at ICES'2K in Los Angeles during August 23 - 25, 2000. In this symposium, 23 speakers with research interests spanning fields as diverse as traditional mechanics, physics, chemistry and materials science have given talks at this symposium. The topics of discussion were focused on sub-continuum modeling of the mechanics of materials, taking into account the atomic structure of solid materials. The main motivation of the symposium was the realization of the limitations of current continuum mechanics modeling approaches (e.g. the finite element method (FEM)) to describe the behavior of materials at scales smaller than tens of microns. The speakers represented the international scientific community in different countries, and utilized diverse simulation and modeling tools for sub-continuum systems. The discussions covered *Ab Initio* quantum simulations (e.g., density functional theory and tight-binding methods), atomistic simulations using empirical many-body interatomic potentials, Monte Carlo methods, mesoscopic statistical and dislocation dynamics, and advanced continuum field equation approaches. In this article, we provide a perspective on the variety of methods presented at the symposium, and a vision for future developments in multiscale simulations for nano- and micro-mechanics of materials.

[1] Mechanical and Aerospace Engineering Department
University of California, Los Angeles
Los Angeles, CA 90095-1597
[2] Division of Mechanics and Computation
Department of Mechanical Engineering
Stanford University
Stanford, CA 94305-4040

1 Introduction

Continuum methods of modeling the behavior of materials have dominated the research scene for over a century. Successful engineering designs have been based on continuum conservation equations, supplemented by a set of phenomenological relationships (or constitutive equations, CEs') between cause and effect (e.g. force and motion, or stress and strain, etc.) Because conservatism is embodied in most engineering designs, such an approach has been successful in designing large-scale structures and components, where the exact knowledge of materials response is not essential. The underlying physical principles behind CEs' are grounded in the statistical mechanics of atomic scale processes. These are captured in the CEs' as macroscopic thermodynamic averages. Within this approach, all atomic scale dynamics and defect evolutions are implicitly averaged over time and space so that the CEs' represent the mechanical behavior of materials over long time and large length scales. Here, the time and length scales are those of typical defects, which determine the mechanical properties: point defects, dislocations, interfaces and grain boundaries. Therefore, continuum ana lyses would be valid only for large enough systems that include a substantial number of defects. Continuum approaches begin to fail as the system size approaches the average separation distance in between defects. At small length scales representative of nano- and micro-engineered material systems, continuum models are not flexible enough to accommodate individual atomic scale processes. While the nano-scale is the length scale of individual atoms and defects (i.e. $1-10\ nm$), and the micro-scale represents the length-scale of typical microstructure (i.e. $0.1-1\ \mu m$), the meso-scale is a typical length scale in which the defect-interface interaction and individual defect dynamics become significant (i.e. $1-100\ \mu m$).

Recently, the confluence of a number of factors has begun to upset the continuum paradigm of engineering de-

sign and analysis. First and foremost are the myriad of experimental observations on the mechanical behavior of materials that cannot be readily explained within the continuum mechanics framework: dislocation patterns in fatigue and creep, surface roughening and crack nucleation in fatigue, the inherent inhomogeneity of plastic deformation, the statistical nature of brittle failure, plastic flow localization in shear bands, and the effects of size, geometry and stress state on the yield properties. Second, while CEs' represent experimental data in some space defined by temperature, stress state, strain rate and material conditions, scientists and engineers have never been comfortable in extending the range of experimentally-derived CEs' without excessive conservatism. If there is no physical understanding, one can simply never be sure about the behavior of materials under unanticipated conditions outside the measured range. Third, the engineering world has shrunk down to small length scales! It is challenging to design engineering systems in the range of nanometers that are anticipated in new generations of computers, electronics, photonics and drug delivery systems. Urgent problems in computer technology depend on understanding failure mechanisms of nano-wires connecting chips in the sub-micron length scale. At the same time, the technology of Micro-Electro-Mechanical Systems (MEMS) has begun to reach the stage where physical understanding of the mechanical behavior will determine the reliability of developed products. There is considerable effort to design ultra-strong and ultra-ductile materials by utilizing the mechanical properties of nano-layers. In high-payoff, high-risk technologies (e.g. nuclear and aerospace), the effects of aging and severe environments on failure mechanisms cannot be left to conservative factor-of-safety approaches to design, but require thorough mechanistic analysis of materials degradation in anticipated environments. All these examples point to the need for a physically-based approach to performance analysis of such small engineering structures. The challenge is great, because neither statistical nor continuum mechanics are reliable in every case. For example, one single nano-void can cause failure of an interconnect on an IC board. Statistical mechanics cannot adequately address this situation, because the law of large numbers is not obeyed. Fourth, the sophistication of computer hardware and software is increasing at an astonishing speed, and large-scale computing is becoming far more accessible than just a few years ago. Today, a cluster of dozens of PCs, linked by network hardware, can cost as little as $30,000 and out-perform supercomputers that used to cost in the millions. Such accessibility is encouraging scientists and engineers to develop efficient numerical methods for modeling complex physical phenomena in materials, without much need for simplified analytical solutions of excessively unrealistic material representations. Computational modeling of materials behavior has begun to complement the traditional theory and experimental approaches of research. Finally and interestingly, the channels of communications between engineers and scientists of uncommon backgrounds are becoming ever more common! In recent technical meetings and conferences one finds mechanical engineers and continuum mechanicians discussing the same issue with materials scientists, physicists and chemists. This barrierless attitude is promoting a sense of creativity and unprecedented fundamental focus in the mechanics of materials field.

An alternative to continuum analysis is atomistic modeling and simulation, in which individual atoms are explicitly followed during their dynamic evolution. Even though this explicit modeling of atomic structures can trace all details of atomic-scale processes, it has its own set of limitations. These are time and length scale limitations from both small and large directions. Since atomistic modeling methods describe atoms explicitly, time scales are on the order of 10^{-15} second (or 1 $fsec$) and length scales on the order fo 10^{-10} m (or 1 $\AA$). As a result of these very small time and length scales, typical atomistic simulations are limited to very small systems over very short times. Even though computing power has been rapidly increasing, brute force simulations using atomistic modeling methods cannot describe systems much larger than 1 μm (billions of atoms) or longer than 1 *msec* (billions of $fsec$ time steps).

The multiscale modeling (MMM) paradigm is based on the realization that continuum and atomistic analysis methods are complementary. At meso-scales (i.e. those *i*n between continuum and atomistic), continuum analyses start to break down, and atomistic methods begin to reach their inherent time and length-scale limitations. Mesoscopic simulation methods are being currently developed to bridge this critical gap in between the extremes of length scales. At the bottom end of the length scales within atomistic simulation methods lies quantum mechanics. Here, components of atoms (e.g. electrons and nucleons) can be explicitly described, albeit with various degrees of approximations. However, quantum sim-

ulation methods require $10^5 - 10^6$ times more computing resources than classical atomistic simulations. Thus, and so far, such methods are limited to atomic systems of a few hundred atoms. It is important to point out that at nano-scales, materials properties are closely coupled so that electronic and chemical properties are strong functions of mechanical deformations. This is evident in the coupling between the band gap and bending strain of SiC nano-tubes, for example (1). Such realization may be opening the door for many and novel nano device applications, where chemo-mechanics and physico-mechanics must be integrated from the start.

The traditional gap between atomistic simulation methods and continuum mechanics has presented significant challenges to the scientific community. When the length-scale cannot be accessed by either continuum methods because it is too small for averaging, or the atomistic methods because it is too large for simulations on present day computers, these two approaches become inadequate. Two possible solutions have emerged so far to this challenge. Instead of simulating the dynamics of atomic systems, one can just study the dynamics of *defect ensembles* in the material. In this innovative strategy, the problem becomes computationally tractable without loss of rigor. Examples of this approach are the dynamical simulations of interacting cracks in brittle materials, or dislocations in crystalline materials. It is noted that the development of dislocation (or defect) dynamics follows from the continuum theory of elasticity, with additional limitations at atomic length scales. Recently, a surge in interest towards understanding the physical nature of plastic deformation has developed. This interest is motivated by the extensive experimental evidence which shows that the distribution of plastic strain in materials is fundamentally heterogeneous ((2)-(4)). Because of the complexity of dislocation arrangements in materials during plastic deformation, an approach, which is based on direct numerical simulations for the motion and interactions between dislocations is now being vigorously pursued. The idea of computer simulation for the interaction between dislocation ensembles is a recent one. During the past decade, the approach of cellular automata was first proposed by Lepinoux and Kubin(5), and that of Dislocation Dynamics by Ghoniem and Amodeo (6)-(12). These early efforts were concerned with simplifying the problem by considering only ensembles of infinitely long, straight dislocations. The method was further expanded by a number of researchers ((13)-(17)), showing the possibility of simulating reasonable, albeit simplified dislocation microstructure. To understand more realistic features of the microstructure in crystalline solids, Kubin, Canova, DeVincre and coworkers ((18)-(25)) have pioneered the development of 3-D lattice dislocation dynamics. More recent advances in this area have contributed to its rapid development (e.g. (26)-(28), and (29)-(31)).

The second solution to the *mesoscale* problem has been based on statistical mechanics approaches (32)-(38). In these developments, evolution equations for statistical averages (and possibly for higher moments) are to be solved for a complete description of the deformation problem. The main challenge in this regard is that, unlike the situation encountered in the development of the kinetic theory of gases and its subsequent extensions to neutrons, plasmas, photons, etc., the geometry of interacting entities within the system matters. It is not conceivable to pursue such an approach without due consideration to the geometry of dislocations and cracks, and to the confinement of their motion on specific slip systems, or along specific directions (37).

In this overview article, we briefly outline the status of research in each component that make up the MMM paradigm for modeling nano- and micro-systems: Quantum Mechanics (QM), Molecular Dynamics (MD), Monte Carlo (MC), Dislocation Dynamics (DD) and Statistical Mechanics (SM). Time and length scale hierarchies, along with a brief classification of computational methods for nano- and micro-systems, are shown in FIG. (1). The current overview is not intended to be exhaustive, but is designed to give the reader an informed level of understanding of the various components of research in MMM, with selected examples to illustrate what is being studied now. Since several of these topics have been addressed within the symposium, we build on the structure of this emerging field, and introduce the papers contained in this special issue. We will finally attempt to project a possible vision for future developments in this emerging field.

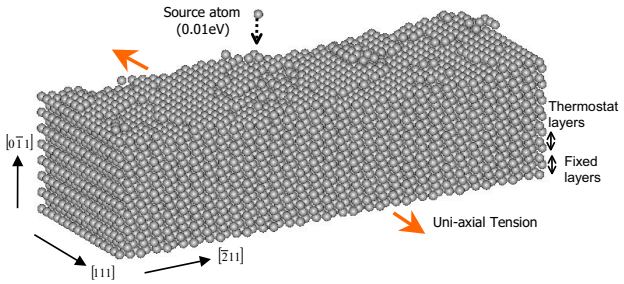

Figure 1 : Schematic illustration of the Multi-scale Materials Modeling (MMM) Hierarchy

2 An Overview of Computational Nano- & Micro-mechanics

2.1 Quantum Mechanics - QM

In recent years, several accurate quantum molecular dynamics schemes have emerged. In these methods, forces between atoms are explicitly computed at each time step within the Born-Oppenheimer approximation (39). The dynamic motion for ionic positions are still governed by Newtonian or Hamiltonian mechanics, and described by molecular dynamics. The most widely known and accurate scheme is the Car-Parrinello (CP) molecular dynamics method (40), where the electronic states and atomic forces are described using the ab-initio density functional method (usually within the local density approximation (LDA)). While such ab-initio MD simulations can now be performed for systems consisting of a few hundred atoms, there is still a vast range of system sizes for which such calculations start to stretch the limits of present day computational resources and become intractable. In the intermediate regimes, between large scale classical MD and quantum (CP) dynamics methods, semi-empirical quantum simulation approaches cover an important system size range where classical potentials are not accurate enough and ab-initio computations are not feasible. The tight-binding molecular dynamics (TBMD) (41) approach thus provides an important bridge between accurate ab-initio quantum MD and classical MD methods.

In the most general approach of full quantum mechanical descriptions of materials, atoms are represented as a collection of quantum mechanical particles, nuclei and electrons, governed by the Schrödinger equation:

$$H\,\Phi\{R_I, r_i\} = E_{tot}\Phi\{R_I, r_i\} \tag{1}$$

With the full quantum many-body Hamiltonian operator:

$$H = \sum \frac{P_I^2}{2M_I} + \sum \frac{Z_I Z_J e^2}{R_{IJ}} + \sum \frac{p_i^2}{2me} + \sum \frac{e^2}{r_{ij}} - \sum \frac{Z_I e^2}{|R_I - r_i|} \tag{2}$$

Where R_I and r_i are nuclei and electron coordinates, respectively. Using the Born-Oppenheimer approximation, the electronic degrees of freedom are assumed to follow adiabatically the corresponding nuclear positions, and the nuclei coordinates become classical variables. With this approximation, the full quantum many-body problem is reduced to a quantum many-electron problem:

$$H\,(R_I)\Psi(r_i) = E_{el}\Psi(r_i) \tag{3}$$

where,

$$H = \sum \frac{P_I^2}{2M_I} + H\,(R_I) \tag{4}$$

Ab initio (or first principles) methods have been developed to solve complex quantum many-body Schrödinger equations using numerical algorithms (43; 44). Current *ab initio* simulation methods are based on the rigorous mathematical foundations provided by two important works of Hohenberg and Kohn (1963) (43), and Kohn and Sham (1964) (44). Hohenberg and Kohn have developed a theorem stating that the ground state energy (E_{el}) of a many-electron system is a functional of the total electron density, $\rho(r)$, rather than the full electron wave function, $\Psi(r_i)$, thus: $E_{el} : (\Psi(r_i)) \equiv E_{el}(\rho(r))$. The Hamiltonian operator H and Schroedinger equation are given by:

$$H\,(R_I) = \sum \frac{p_i^2}{2me} + \sum \frac{e^2}{r_{ij}} - \sum \frac{Z_I e^2}{|R_I - r_i|} + \sum \frac{Z_I Z_J e^2}{R_{IJ}} \tag{5}$$

$$E_{el}\Psi(r_i) = H\,(R_I)\Psi(r_i) \tag{6}$$

where R_I and r_i are atomic positions and electronic coordinates, respectively. The density functional theory (DFT) is derived from the fact that the ground state total electronic energy is a functional of the total electron density $r(\rho)$. Subsequently, Kohn and Sham have shown that the DFT can be reformulated as a single electron problem with self-consistent effective potential including all the

exchange-correlation quantum effects of electronic interactions:

$$H_1 = \frac{p^2}{2me} + V_H(r) + V_{XC}[r(\rho)] + V_{ion-el}(r), \quad (7)$$

$$r(\rho) = \sum |\Psi_i(r)|^2, \quad (8)$$

$$H_1\Psi_i(r) = \varepsilon_i\Psi_i(r), \quad i = 1,,N_{tot}. \quad (9)$$

This single electron Schrödinger equation is known as Kohn-Sham equation, and the local density approximation (LDA) has been introduced to approximate the unknown effective exchange-correlation potential $V_{XC}[r(\rho)]$. This DFT-LDA method has been very successful in predicting the properties of materials without using any experimental inputs other than the identity (i.e., atomic numbers) of constituent atoms (40; 42). For practical applications, however, the DFT-LDA method has been implemented with a pseudopotential approximation and a plane wave (PW) basis expansion of single electron wave functions. These systematic approximations reduce the electronic structure problem as a self-consistent matrix diagonalization problem. Over the last three decades, the simulation method has been rapidly improved from iterative diagonalization (ID), to Car-Parrinello molecular dynamics (CPMD) (40), to conjugate gradient (CG) minimization methods. CPMD has significantly improved the computational efficiency by reducing the N^3-scaling of ID method down to N^2-scaling. The CG method has further improved the efficiency by an additional factor of 2-3. One of the popular DFT simulation programs is the Vienna *Ab initio* Simulation Package (VASP), which is available through a license agreement (45). For response function analysis (e.g., dielectric tensor, phonon spectrum, stress/strain tensors), the ABINIT code is a well-developed DFT code (46). Another useful DFT simulation program has been developed in C^{++} language (47). In addition to these simulation programs, there is also a commercial package from Molecular Simulation Inc. (48). With these and other widely used DFT simulation packages, the *ab initio* simulation method has been established as a major computational materials research tool (49).

Since the DFT simulation enables us to model a few hundred atoms without any experimental inputs, it provides a powerful tool to investigate nanomaterials with predictive power. Nanomaterials are building blocks of nanotechnology, and it is essential to develop detailed under-

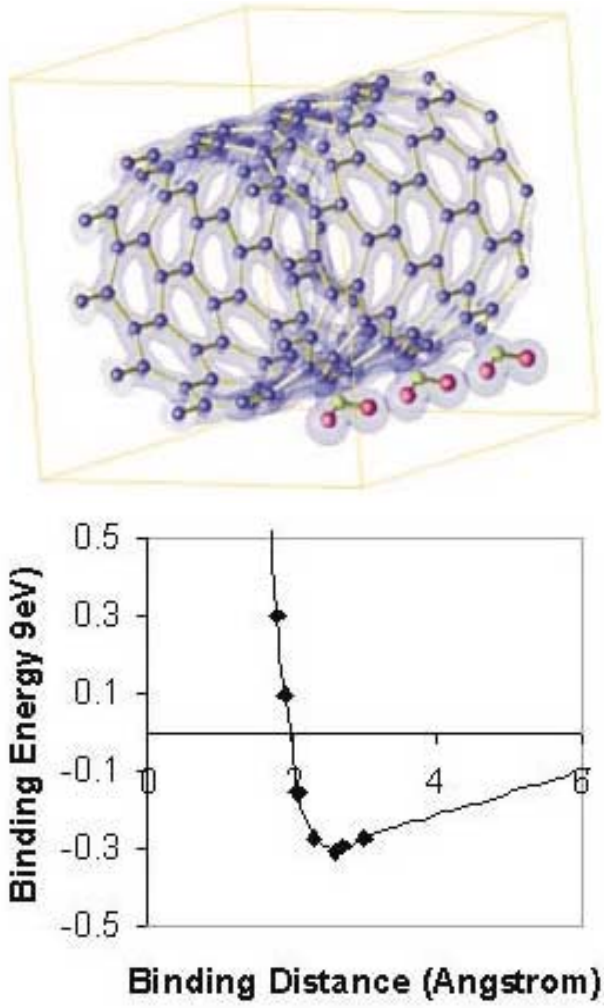

Figure 2 : Top: Total valence electron charge density plot. The value of charge contour is 0.0015 (eV/Å) showing the binding charge between the SWNT (10,0) and the NO_2 molecule. Three units are shown in this figure. Bottom: Binding energy curve for NO_2 interacting with (10,0) SWNT as a function of distance from NO_2 to the nanotube. The solid line curve is a fitting with universal binding curve.

standing of their diverse material properties. However, experimental characterization is very challenging due to extremely small size of nanostructures. Quantum simulations provide a natural solution to this problem complementing the experimental nanomateirals research. Here we illustrate the use of ab initio simulations to the study of carbon nanotube gas sensor applications. Recent experiments have shown that carbon nanotubes can change their electronic properties due to the presence of very small amount of gas molecules (e.g., NO_2, NH_3, or O_2). The underlying mechanism of the gas molecule detection was proposed to be the adsorption of the molecules on the nanotube surface and accompanying charge transfer between the molecules and nanotube.

To test this assumption, Peng and Cho have performed DFT simulations of gas molecule - carbon nanotube systems. FIG. (2) shows the results of DFT simulatiosn for NO_2-(10,0) nanotube system. Three NO_2 molecules are shown at the lower right corner of the left panel, and the molecule-nanotube binding energy curve is shown in the right panel. The energy curve shows that there is an attractive interaction between NO_2 molecule and the nanotube with 0.34 eV binding energy. The analysis of electronic structure change shows that there is a net electron transfer (about 0.1 eV) from nanotube to NO_2 molecule leading to p-type doping in the semiconducting (10,0) nanotube. This example illustrates that quantum simulations can model detailed electronic structures, binding configurations, and energetics of nanoscale materials leading to detailed mechanistic understanding of their properties.

2.2 Classical Molecular Dynamics - MD

Classical molecular dynamics (MD) simulations describe the atomic scale dynamics of a system, where atoms and molecules move while simultaneously interacting with many other atoms and molecules in their vicinity. The dynamic evolution of the system is governed by Newton's equations of motion:

$$\frac{d^2R_I}{dt^2} = F_I = -\frac{dV}{dR_I}, \tag{10}$$

which is derived from the classical Hamiltonian of the system:

$$H = \sum \frac{P_I^2}{2M_I} + V(R_I) \tag{11}$$

Each atom moves and acts simply as a rigid particle that is moving in the many-body potential of other similar particles, $V(R_I)$, which can also be obtained from more accurate quantum simulations. The atomic and molecular interactions describing the system dynamics are given by classical many-body force field functions. The atomic interaction energy function $V(R_I)$ can be written in terms of pair and many-body interactions, depending on the relative distances among different atoms (50; 51). Atomic forces are derived as analytic derivatives of the interaction energy functions, $F_I(R_I) = -dV/dR_I$, and are used to construct Hamilton's equations of motion, which are 2^{nd} order, ordinary differential equations. These equations are approximated as finite difference equations, with a discrete time step δt, and are solved by standard time integration algorithms, The simulations can be performed under a variety of physical conditions through discrete time evolution, starting from specified initial condition.

Until the early 1970's, MD simulations utilized simple interatomic potentials, such as the Lennard-Jones potential, to qualitatively model diverse properties of material systems. To model more realistic materials, such as metals and semiconductors with complex many-body interactions, three approaches have emerged: (1) potentials developed on following the Born-Openheimer expansion (e.g. the Pearson (52) and Stillinger-Weber (SW) (53) potentials); (2) potentials that attempt to model the local environment using electron density distributions (e.g. the Embedded Atom Method (EAM) (50; 51)); (3) potentials that introduce the local electronic environment directly into pair potentials (e.g. the Tersoff potential (54)).

The Born-Openheimer expansion expresses the interatomic potential as an infinite sum over pair, triplet, etc. interactions between atoms in the solid, as:

$$\begin{aligned}\Phi_t(r_1, r_2, r_3, \cdots) = &\frac{1}{2!}\sum_{j\neq l} V^{(2)}(r_{ij}) \\ &+ \frac{1}{3!}\sum_{k\neq}\sum_{j\neq i} V^{(3)}(r_{ij}, r_{jk}, r_{ki}) \\ &+ \cdots \frac{1}{n!}\sum_{q\neq}\cdot\cdot\sum_{m\neq}\cdot\cdot\sum_{j\neq l} V^{(n)}(r_{ij}, \cdot\cdot, r_{iq}, \cdot\cdot, r_{mq}, \cdot\cdot)\end{aligned} \tag{12}$$

For covalently-bonded materials, Pearson takes the two-body component to be the Lennard-Jones potential, while triplet interactions are represented by an Axilrod-Teller-type three-body potential (52). The SW potential is an-

other example of the type of potential that is used to effectively deal with the directional nature of bonding in covalent materials. The EAM potential was originally developed for metals by Daw and Baskes (50). In this approach, the energy of an atom in the crystal is divided into two parts: (1) a two-body core-core interaction energy $\Phi_{ij}(r_{ij})$; (3) an additional energy needed to *embed* the atom into the electron system in the lattice $F_i(\overline{\rho}_i)$, where $\overline{\rho}_i$ is the average local electron density. The total configurational energy fo the crystal is written as a sum of these two types of contributions:

$$E = \sum_i \left\{ F_i(\overline{\rho}_i) + \sum_{j \neq i} \frac{1}{2} \Phi_{ij}(r_{ij}) \right\} \tag{13}$$

The embedding energy is usually fit to the form:

$$F_i = A_i E_i^0 \overline{\rho}_i \ln \overline{\rho}_i \tag{14}$$

Where A_i is a constant for atom type i, E_i^0 is its sublimation energy, and $\overline{\rho}_i$ is obtained by functional fits to the electronic configuration surrounding atom i. Based on variations of these EAM and SW potentials, a wide variety of many-body potentials have been proposed and used in classical molecular dynamics simulations. These potentials are expected to work well within the range of physical parameters in which they were constructed. Numerical integration of the equations of motion is performed either by explicit or implicit methods. The simple Euler scheme is not appropriate for MD simulations because of it lacks numerical stability. In the explicit Verlet's leap-frog method, the equation of particle motion is split into two first-order equations:

$$\frac{dx}{dt} = v, \qquad \frac{dv}{dt} = f(x,t) \tag{15}$$

When these equations are discretized and re-combined, one gets for the particle position after a small time increment Δt:

$$x_{n+1} = x_{n-1} + 2\Delta t (v_{n-2} + 2\Delta t f_{n-1}) \tag{16}$$

The Verlet algorithm is very popular in MD simulations because it is stable, memory-efficient, and allows a reasonably large time-step. Another popular implicit integration method for MD simulations is the predictor-corrector scheme, and in particular, the Gear algorithm (55). These techniques are formulated either as multivalue, where higher-order spatial derivatives are carried

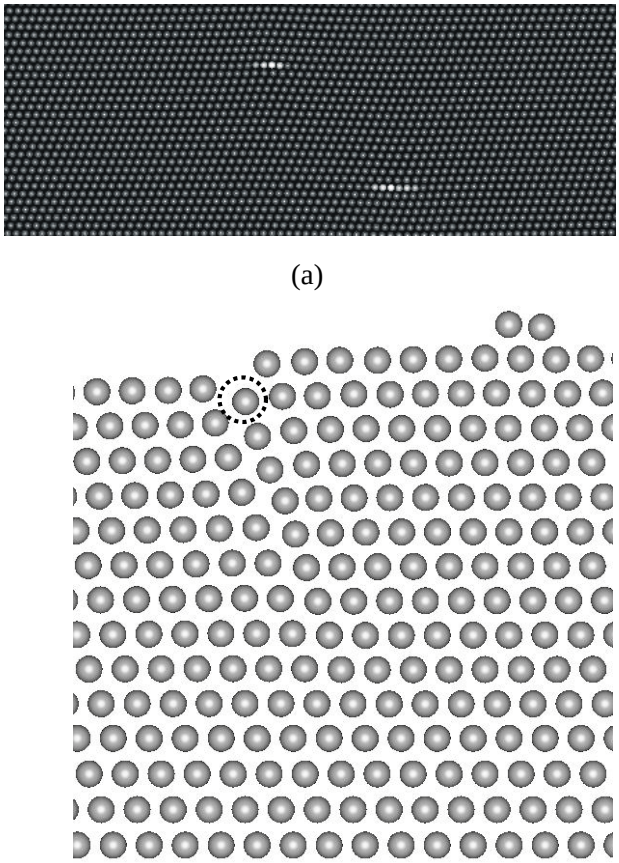

(a)

(b)

Figure 3 : Snapshots of a portion of the (011) cross-section with the relative angle being (a) 45°, and (b) 135°, when the relative velocity is $0.93C_t$ at 45°. The dislocation positions are indicated by the locations of the lighter atoms, and dislocation on the top is positive while the one at the bottom is negative (coutesy of H. Huang)

out, or multi-step, where positions and velocities from several previous time steps are used for prediction.

In standard MD simulations, the number of atoms, simulation volume and total energy are constant, thus time averages are measured in the microcanonical (NVE) ensemble. This is not necessarily desirable, and more often, either an isothermal (NVT) or an isobaric (NVT) microcanonical ensembles are more preferable. Depending on the problem being simulated, algorithms are developed to maintain either constant temperature or constant pressure. In the case of constant temperature simulations, a *thermostat* is used. The crudest thermostat is the Berendsen algorithm, in which the velocities are simply re-scaled as: $\mathbf{v^{n+1}} = \eta\tilde{\mathbf{v}}^{\mathbf{n+1}}$, where:

$$\eta = \sqrt{1 + \frac{\Delta t}{\tau}(\frac{T^*}{T} - 1)} \tag{17}$$

and $T*$ is the isothermal target temperature, $\tilde{\mathbf{v}}$ is the computed velocity, $\mathbf{v}$ the re-normalized velocity and τ & η are parameters. A number of more sophisticated thermostats have also been developed, such as the Anderson thermostat where thermalization is established by random collisions with a bath, the iso-kinetic thermostat where the equations of motion are modified to establish constant average kinetic energy, and its variant: the Nosè-Hoover thermostat that uses the time average of the kinetic energy, rather than its instantaneous value to establish iso-kinetic conditions (56)-(58). In some specialized MD simulations, additional force fields of a long-range nature may be present, such as the situation in studies of ionic crystals, piesoelectric or magnetostrictive materials. Extensions of the simulation methods of plasma have been attempted, in which particle MD simulations are embedded into field solvers on a spatial mesh. Such algorithms are sometimes called the *Particle-Particle-Particle-Mesh*, or (PPPM) algorithms. These algorthims are based on decomposing the problem into two parts. First, the short range forces are computed using particles, then, long range forces are computed using discretized continuum equations, where the particles are *smeared out* over a specified spatial domain.

To illustrate results o MD simulations, we will discuss here the problem of dislocation dipole stability during the dynamic interactions of two dislocations of opposite sign (59)., dislocations are generated by adding two extra (211) planes along the [111] direction to the lower half of the simulation cell for the negative dislocation in the

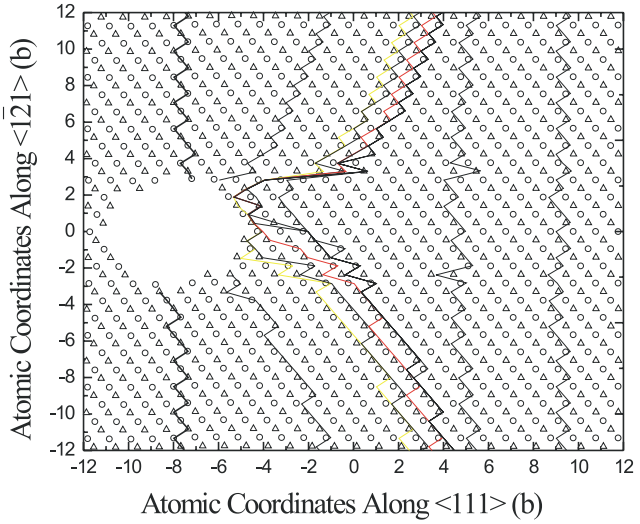

Figure 4 : Atomic positions of a dislocation core at successive time instances, as it passes through a small microvoid in Fe(coutesy of H. Huang)

dipole. The positive dislocation is created by pushing a piston at the speed of 75 m/s. The glide planes of the two dislocations are separated by $14|\mathbf{b}|$, $\mathbf{b}$ being the Burgers vector. During the simulations, the temperature is kept below 35 K, to eliminate the effects of thermal fluctuations. This temperature control is accomplished by applying a Langevin force to atoms in the dynamic region (60). Two snapshots, corresponding to the 45° configuration, at which the relative velocity is $0.93C_t$, where C_t is the speed of sound, and the final 135° configuration, are shown in FIGs (3-a) and (3-b), respectively. The MD studies reported in by Wang, Huang and Woo (59) indicate that, under high speed deformation conditions, two approaching dislocations, which would normally form a stable dipole, may become unstable as a result of the additional kinetic energy involved during the dipole interaction. Another example that illustrates the interaction between high-speed dislocations and voids is shown in FIG. (4). In this work, the process of interaction between high-spped dislocations and micro-voids is simulated with the calssical MD techique. The passage of a dislocation through a small void does not result in dissolution of the microvoid, because of the short time scale in MD simulations. However, successive passages of the dislocation and its cutting of microvoids eventually results in the destruction of the microvoid.

2.3 Kinetic Monte Carlo - KMC

The Monte Carlo (MC) method refers to any stochastic technique, which investigates problems by sampling from random distributions, and utilize concepts of probability theory. These techniques are now routinely applied in almost every field, from biology to nuclear physics to social studies. The MC method is simply a statistical method for solving deterministic or probabilistic problems. A computer simulation represents a physics experiment carried out numerically.

The generation of random numbers uniformly distributed over the interval $[\in (0,1)]$ is a fundamental aspect of Monte Carlo simulations. Frequently, the mid-square or the linear/multiplicative congruential method is used in computer algorithms to generate a sequence of random numbers(61). MC simulations generally require random numbers generated according to specific statistical distributions. General purpose algorithms are available for generating random numbers following arbitrary given distribution functions. One of the methods for generation of random numbers according to a given distribution function is the inversion method, which is only effective for relatively simple distributions. The idea is that, if the distribution function is normalized to obtain a probability density function (PDF) $p(x)$, we can obtain the probability that the random variable x' is less than an arbitrary x by integrating the PDF analytically from the minimum value to x. The integral of the (PDF) is called the cumulative distribution function (CDF) $C(x)$. When the CDF is equated to a uniformly distributed random number ρ, $C(x) = \rho$, the resulting solution for x gives the desired distribution function, thus:

$$x = C^{-1}(\rho) \tag{18}$$

Since each random number ρ results in one value for x, the method is very efficient. If the PDF $p(x)$ cannot be easily inverted analytically, sampling can be performed by the Von Neumann rejection technique. In this method, a trial value, x_{trial} is chosen randomly, and it is accepted with a probability proportional to $p(x)$. First, a pair of random numbers ρ_1 and ρ_2 are generated. A trial value of x, is the obtained as:

$$x_{\text{trial}} = x_{\min} + (x_{\max} - x_{\min})\rho_1 \tag{19}$$

If $f(x_{\text{trial}}) \geq \rho_2 M$, where M is the maximum value that the function can reach over the interval $[x_{\min}, x_{\max}]$, then x_{trial} is accepted; otherwise the procedure is repeated until a trial value is accepted. The rejection technique is inefficient when the distribution function has one or more large peaks. Another popular methods is known as importance sampling, and is a combination of the previous two methods. In this technique, we replace the original distribution function, $p(x)$, by an approximate form, $\tilde{p}(x)$, for which the inversion method can be applied. Then we obtain the trial values for x with the inversion technique following $p'(x)$, and accept the trial values with the probability proportional to the weight w:

$$w = \frac{p(x)}{\tilde{p}(x)} \tag{20}$$

It can be shown that the rejection technique is just a special case of the importance sampling, where $p'(x)$ is a constant(62).

In some applications of the MC method, the number of new configurations available to the system at any MC step is finite and enumerable. The configuration space is discrete, rather than continuous. In other words, at each MC step, we can determine all the phenomena and the rates at which they occur, i.e. all the changes that the system can possibly experience. Therefore, we need not perform a random change to the system at each MC step and then accept or reject that change on the basis of a specified criterion. Based on the relative rates associated with each change, we can choose and execute a single change to the system from the list of all possible changes at each MC step. This is the general idea of the Kinetic Monte Carlo (KMC) method. KMC methods have been employed in studies of radiation damage since the 1970s ((63), (64), (65)). They can take into account simultaneously many different microscopic mechanisms, covering very different time scales that are difficult to handle with other atomistic simulation techniques.

In order to perform a KMC simulation, the first step is to tabulate the rate at which each event or phenomenon will occur anywhere in the system, r_i. The probability of choosing an event is defined as the rate at which the event occurs relative to the sum of the rates of all possible events. Once an event is chosen, the system is changed appropriately, and the list of events that can occur at the next KMC step is updated. Therefore, at each KMC step, one event denoted by m is randomly chosen from all of the M events that can possibly occur at that step, as follows:

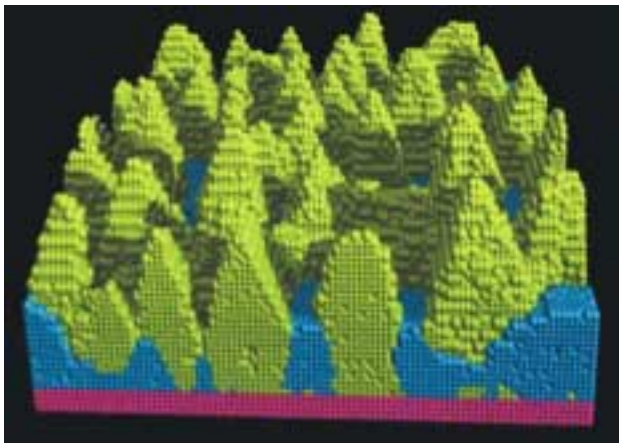

Figure 5 : Results of KMC simulations for thin film growth on a substrate showing columnar growth (courtesy of H. Huang)

$$\sum_{i=0}^{m-1} r_i / \sum_{i=0}^{M} r_i < \xi < \sum_{i=0}^{m} r_i / \sum_{i=0}^{M} r_i \tag{21}$$

where r_i is the rate at which event i occurs ($r_0 = 0$) and ξ is a random number uniformly distributed in the range $[\in (0,1)]$. After an event is selected and carried out, the total number of possible events, M, and the sequence in which the events are labeled, are updated (66). In conventional KMC simulations, a fixed time increment is chosen such that at most one event happens during each time step(67). However, this approach is inefficient since in many time steps, no events will happen. An alternative technique, introduced by Bortz, *et al*.(68) ensures that one event occurs somewhere in the system, and the time increment itself can be determined at each step. In this approach, since one event occurs at each simulation step and different events occur at different rates, the time increment, dt, corresponding with each step is dynamic and stochastic:

$$dt = -\ln(\eta) / \sum_{i=1}^{M} r_i \tag{22}$$

Where η is a random number evenly distributed the range $[\in (0,1)]$. This method is particularly useful in cases where the events occur at very different time scales, and the fastest events are only possible in certain rare situations. FIG. (5) below illustrates the final stages of columnar thin film growth during Physical Vapor Deposition (PVD) utilizing the KMC technique (69), (70). Another example, which illustrates the power on KMC computations in predictions of experimental observations is shown in FIG. (6). In this example, the motion of Self-Interstitial Atom (SIA) clusters is simulated in crystals containing dislocations. The internal field of dislocations has a profound effect on the motion of such clusters. As a result of the stress field of dislocations, these clusters execute two types of motions: (1) random along highly-packed orientations; (2) drift motion by elastic interaction with dislocations. The elastic interaction results in cluster rotation, leading to decoration of dislocation segments, pinning of mobile clusters and dislocation loop raft formation. FIG. (6) shows various stages of computer simulation (71), while FIG. (7) shows TEM experimental observations of dislocation decoration in irradiated Mo (72).

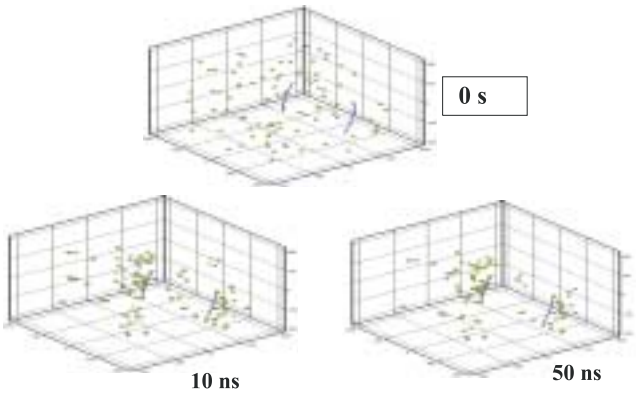

Figure 6 : Results of KMC simulations for SIA cluster agglomeration and interaction near dislocation segments

2.4 Dislocation Dynamics - DD

Because the internal geometry of imperfect crystals is very complex, a physically-based description of plastic deformation can be very challenging. The topological complexity is manifest in the existence of dislocation structures within otherwise perfect atomic arrangements. Dislocation loops delineate regions where large atomic displacements are encountered. As a result, long-range elastic fields are set up in response to such large, localized atomic displacements. As the external load is maintained, the material deforms plastically by generating more dislocations. Thus, macroscopically observed plastic deformation is a consequence of dislocation generation and motion. A closer examination of atomic po-

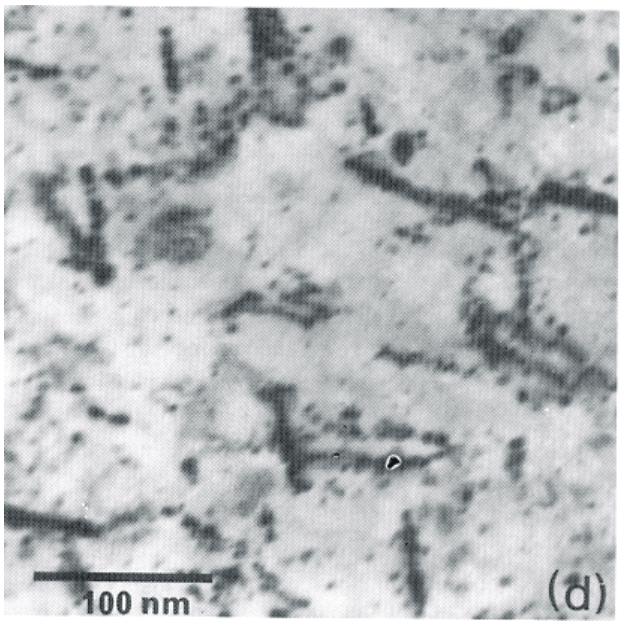

Figure 7 : Experimental TEM observations of SIA clusters decorating dislocations in irradiated Mo

sitions associated with dislocations shows that large displacements are confined only to a small region around the dislocation line (i.e. *the dislocation core*). The majority of the displacement field can be conveniently described as elastic deformation. Even though one utilizes the concept of dislocation distributions to account for large displacements close to dislocation lines, a physically-based plasticity theory can paradoxically be based on the theory of elasticity! Since it was first introduced in the mid-eighties (73), (74), Dislocation Dynamics (DD) has now become an attractive tool for investigations of both fundamental and collective processes that constitute plastic deformation of crystalline materials. In its early versions, the collective behavior of dislocation ensembles was determined by direct numerical simulations of the interactions between infinitely long, straight dislocations. The numerical accuracy and limitations of the 2-D description of dislocation ensemble evolution has been examined in considerable detail (e.g. (75)-(83)). Although the numerical issues of stability, accuracy, convergence and field approximations have been largely resolved in the 2-D case, it has been realized that the fundamental physical nature of dislocation loops, being 3-D space curves, makes progress with rigorous 2-D simulations rather difficult without additional ad-hoc rules of close-range interactions. Such realization prompted several research groups to consider extensions of the DD methodology to the more physical, yet considerably more complex conditions of 3-D DD computer simulations of plastic deformation.

The starting point in DD simulations is a description of the elastic field of dislocation loops of arbitrary shapes. The stress σ tensor of a closed dislocation loop in an isotropic crystal is given by deWit (1960) as (84):

$$\sigma_{ij} = \frac{\mu}{4\pi}\oint_C \left[\frac{1}{2}R_{,mpp}\left(\varepsilon_{jmn}dl_i + \varepsilon_{imn}dl_j\right) + \frac{1}{1-\nu}\varepsilon_{kmn}\left(R_{,ijm} - \delta_{ij}R_{,ppm}\right)dl_k\right] \tag{23}$$

Where μ & ν are the shear modulus and Poisson's ratio, respectively, $\mathbf{b}$ is Burgers vector of Cartesian components b_i. The radius vector $\mathbf{R}$ connects a source point on the loop to a field point, with Cartesian components R_i, successive partial derivatives $R_{,ijk\ldots}$, and magnitude R. The line integrals are carried along the closed contour C defining the dislocation loop, of differential arc length $d\mathbf{l}$ of components dl_k. The line integral is discretized, and the stress field of dislocation ensembles is obtained by a summation process over line segments. Recently, Ghoniem, Huang and Wang (85)-(88) have shown that if dislocation loops are discretized into curved parametric segments, one can obtain the field by numerical integration over the scalar parameter that represents the segment. If one of these segments is described by a parameter ω that varies, for example, from 0 to 1 at end nodes of the segment. The segment is fully determined as an affine mapping on the scalar interval $\in [0,1]$, if we introduce the tangent vector $\mathbf{T}$, the unit tangent vector $\mathbf{t}$, the unit radius vector $\mathbf{e}$, as follows: $\mathbf{T} = \frac{d\mathbf{l}}{d\omega}$, $\mathbf{t} = \frac{\mathbf{T}}{|\mathbf{T}|}$, $\mathbf{e} = \frac{\mathbf{R}}{R}$. Let the Cartesian orthonormal basis set be denoted by $\mathbf{1} \equiv \{\mathbf{1}_x, \mathbf{1}_y, \mathbf{1}_z\}$, $\mathbf{I} = \mathbf{1} \otimes \mathbf{1}$ as the second order unit tensor, and $\otimes$ denotes tensor product. Now define the three vectors $(\mathbf{g}_1 = \mathbf{e},\ \mathbf{g}_2 = \mathbf{t},\ \mathbf{g}_3 = \mathbf{b}/|\mathbf{b}|)$ as a covariant basis set for the curvilinear segment, and their contravariant reciprocals as: $\mathbf{g}^i \cdot \mathbf{g}_j = \delta^i_j$, where δ^i_j is the mixed Kronecker delta and $V = (\mathbf{g}_1 \times \mathbf{g}_2) \cdot \mathbf{g}_3$ the volume spanned by the vector basis, as shown in FIG. (8). The differential stress field is given by:

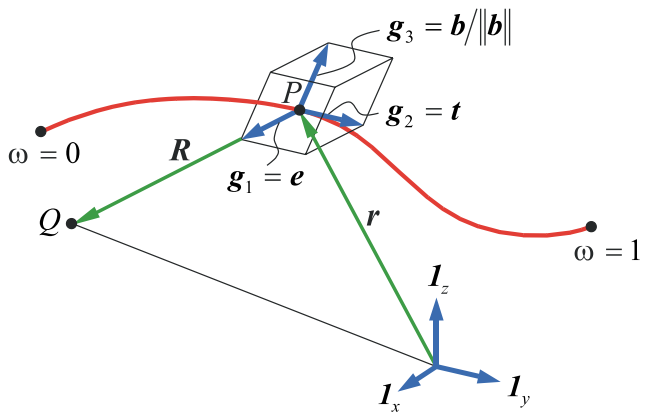

Figure 8 : Parametric Representation of Dislocation Segments

$$\frac{d\sigma}{d\omega} = \frac{\mu V|\mathbf{T}|}{4\pi(1-\nu)R^2}\left\{\left(\mathbf{g}^1\otimes\mathbf{g}_1+\mathbf{g}_1\otimes\mathbf{g}^1\right)\right.$$
$$\left.+(1-\nu)\left(\mathbf{g}^2\otimes\mathbf{g}_2+\mathbf{g}_2\otimes\mathbf{g}^2\right)-(3\mathbf{g}_1\otimes\mathbf{g}_1+\mathbf{I})\right\} \quad (24)$$

Once the parametric curve for the dislocation segment is mapped onto the scalar interval $\{\omega\in[0,1]\}$, the stress field everywhere is obtained as a fast numerical quadrature sum (85). The Peach-Kohler force is then obtained on any other segment point as (86):

$$\mathbf{F}_{PK} = \sigma\cdot\mathbf{b}\times\mathbf{t} \quad (25)$$

The self-force is obtained from knowledge of the local curvature at the point of interest. The variational form of the governing equation of motion of a single dislocation loop is given by (86):

$$\int_\Gamma \left(F_k^t - B_{\alpha k}V_\alpha\right)\delta r_k\,|d\mathbf{s}| = 0 \quad (26)$$

Here, F_k^t are the components of the resultant force, consisting of the Peach-Koehler force (87) $\mathbf{F}_{PK}$ (generated by the sum of the external and internal stress fields), the self-force $\mathbf{F}_s$, and the Osmotic force $\mathbf{F}_O$ (in case climb is also considered(86)). The resistivity matrix (inverse mobility) is $B_{\alpha k}$, V_α are the velocity vector components, and the line integral is carried along the arc length of the dislocation $d\mathbf{s}$. To simplify the problem, let us define the following dimensionless parameters:

$$\mathbf{r}^* = \frac{\mathbf{r}}{a}, \qquad \mathbf{f}^* = \frac{\mathbf{F}}{\mu a}, \qquad t^* = \frac{\mu t}{B}$$

Here, a is lattice constant, μ the shear modulus, and t is time. Hence EQN. 26 can be rewritten in dimensionless matrix form as:

$$\int_{\Gamma^*}\delta\mathbf{r}^{*\top}\left(\mathbf{f}^* - \frac{\mathbf{dr}^*}{dt^*}\right)|d\mathbf{s}^*| = 0 \quad (27)$$

Here, $\mathbf{f}^* = [f_1^*, f_2^*, f_3^*]^\top$, and $\mathbf{r}^* = [r_1^*, r_2^*, r_3^*]^\top$, which are all dependent on the dimensionless time t^*. Following reference (86), a closed dislocation loop can be divided into N_s segments. In each segment j, we can choose a set of generalized coordinates q_m at the two ends, thus allowing parameterization of the form:

$$\mathbf{r}^* = \mathbf{CQ} \quad (28)$$

Here, $\mathbf{C} = [C_1(\omega), C_2(\omega), ..., C_m(\omega)]$, $C_i(\omega), (i = 1,2,...m)$ are shape functions dependent on the parameter $(0\le\omega\le 1)$, and $\mathbf{Q} = [q_1, q_2, ..., q_m]^\top$, q_i are a set of generalized coordinates. Now substitute EQN.28 into EQN.27, we obtain:

$$\sum_{j=1}^{N_s}\int_{\Gamma_j}\delta\mathbf{Q}^\top\left(\mathbf{C}^\top\mathbf{f}^* - \mathbf{C}^\top\mathbf{C}\frac{d\mathbf{Q}}{dt^*}\right)|d\mathbf{s}| = 0 \quad (29)$$

Let,

$$\mathbf{f}_j = \int_{\Gamma_j}\mathbf{C}^\top\mathbf{f}^*\,|d\mathbf{s}|, \qquad \mathbf{k}_j = \int_{\Gamma_j}\mathbf{C}^\top\mathbf{C}\,|ds|$$

Following a similar procedure to the FEM, we assemble the EOM for all contiguous segments in global matrices and vectors, as:

$$\mathbf{F} = \sum_{j=1}^{N_s}\mathbf{f}_j, \qquad \mathbf{K} = \sum_{j=1}^{N_s}\mathbf{k}_j$$

then, from EQN 29 we get,

$$\mathbf{K}\frac{d\mathbf{Q}}{dt^*} = \mathbf{F} \quad (30)$$

EQN. 30 represents a set of ordinary differential equations, which describe the motion of an ensemble of dislocation loops as an evolutionary dynamical system. Generally, two numerical time integration methods are available for solving this set of equations: the implicit and the explicit classes of procedures. We will later discuss

the accuracy and stability issues associated with each scheme.

It is now recognized by many that fundamental studies of plasticity requires levels of temporal and spatial resolution concomitant with the question at hand. For instance, atomic spatial resolution and pico-second temporal resolution are both required for studies of the intrinsic properties of single dislocations, or for single dislocation interaction with atomic size defects. However, development of constitutive equations of polycrystalline materials does not necessarily require such high level of resolution, mainly because statistical averaging takes care of minute details. There is an enormous range of problems in-between, spanning deformation behavior of nano-, micro-, and single crystal materials, all the way up to polycrystalline material deformation. A number of numerical simulation approaches have been under development in recent years, with emphasis on resolution of specific dislocation interaction mechanisms, or on the collective behavior of dislocation ensembles. These approaches differ mainly in the representation of dislocation loop geometry, the manner by which the elastic field and self energies are calculated, and some additional details related to how boundary and interface conditions are handled. Nonetheless, the methods can be differentiated, and may be categorized in one of the following:

1. The Lattice Method:(89)-(98):
   Here, straight dislocation segments (either pure screw or edge in the earliest versions , or of a mixed character in more recent versions,) are allowed to jump on specific lattice sites and orientations.

2. The Force Method:(99)-(100):
   Straight dislocation segments of mixed character are moved in a rigid body fashion along the normal to their mid-points . No information of the elastic field is necessary, since explicit equations of interaction forces, developed by Yoffe (101) are directly used.

3. The Differential Stress Method:(102) -(104):
   The stress field of a differential straight line element on the dislocation is computed and integrated numerically to give the necessary Peach-Koehler force . The Brown procedure (105) is then utilized to remove the singularities associated with the self force calculation.

4. The Parametric Method: (85)-(88), (107):
   Dislocation loops are divided into contiguous segments represented by parametric space curves. The equations of motion for nodal attributes (e.g. position, tangent and normal vectors) are derived from a variational energy principle, and once determined, the entire dislocation loop can be geometrically represented as a continuous (to second derivative) composite space curve. The Parametric Dislocation Dynamics (PDD) methodology is based on two main principles that are often employed in modern numerical methods of continuum mechanics (i.e. the Finite Element Method **FEM**)(86),(88). The first is some energy-based variational principle that would allow one to derive the equations of motion (EOM) of a *reduced set* of Degrees Of Freedom (DOF) representing the system. The second principle is a *kinematic* assumption regarding how the displacement or strain field is assumed to vary in a specified region of the continuum. To draw the analogy, a minimization of the Gibbs free energy of a single loop upon its virtual motion in the external and internal field results in the EOM, while assuming spline functions between some fixed nodes on the dislocation loop corresponds to the kinematic assumption of continuum mechanics.

5. The Phase Field Microelasticity Method:(108)-(110):
   Based on Khachaturyan-Shatalov(KS) reciprocal space theory of the strain in an arbitrary elastically homogeneous system of misfitting coherent inclusions embedded into the parent phase, a consideration of individual segments of all dislocation lines is not required. Instead, the temporal and spatial evolution of several density function profiles (fields) are dealt with.

The vector forms in EQN. 24 can be integrated for complex-shape loop ensembles, by application of the fast sum method (85). In typical DD computer simulations, the shape of loop ensembles is evolved using equations of motion for generalized coordinates representing the position, tangent, and normal vectors of nodes on each loop. FIG. (9) shows the results of such computations for simulation of plastic deformation in single crystal copper under the action of a slow stress ramp. The initial dislocation density of $\rho = 2 \times 10^{13}\ m^{-2}$ has been divided into 68 complete loops. Each loop contains a random number of straight glide and superjog segments. When a gener-

ated or expanding loop intersects the simulation volume of 3 μm side length, the segments that lie outside the simulation boundary are periodically mapped inside the simulation volume to preserve translational strain invariance, without loss of dislocation lines. The initially straight, segmented dislocation microstructure evolves under an applied stress σ_{xx} =120 MPa in FIG. 6-a, and 165 MPa in FIG. 6-b (88).

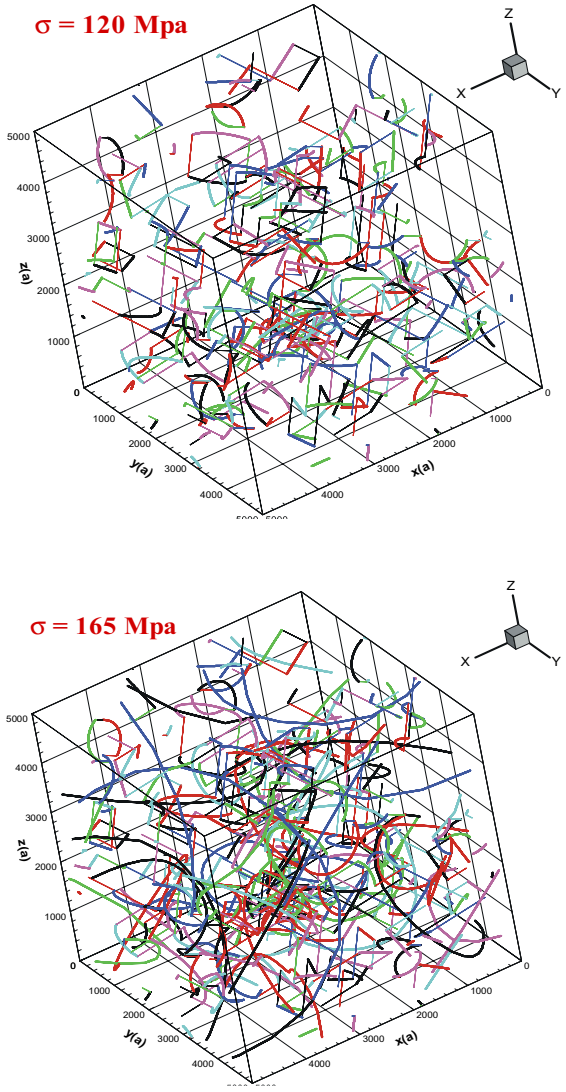

Figure 9 : Results of computer simulations for dislocation microstructure deformation under uniaxial applied stress

2.5 Statistical Mechanics - SM

A number of approaches for a physical description of inhomogeneous plastic deformation, and following concepts of statistical mechanics, have emerged during the past two decades. The fundamental difficulty here is that dislocations, unlike particles, are linear objects of considerable topological complexity. Hence, when concepts of statistical mechanics and the theory of rate processes are used, some level of phenomenological description is unavoidable. We present here, as one example, a reaction-transport approach to Persistent Slip Band (PSB) formation. In this approach, the system is supposed to be composed of nearly immobile dislocations of the forest, and mobile dislocations, moving on their glide planes. Coupled rate equations for corresponding dislocation densities are derived in the spirit of the dislocation dynamical models derived for example by Ghoniem et al. (111) for creep, or by Walgraef and Aifantis(32) and Kratochvil (112) for dislocation microstructure formation in fatigue.

The static dislocation density, formed by the immobilized dislocations of the forest, sub-grain walls or boundaries, is defined as ρ_s, and the mobile dislocation density for dislocations gliding between obstacles is defined as ρ_m. For simplicity, we will consider first systems oriented for single slip. Hence, the mobile dislocation density, ρ_m is divided into two sub-family densities representing dislocations gliding in the direction of the Burgers vector (ρ_m^+) or in the opposite direction (ρ_m^-) (with $\rho_m = \rho_m^+ + \rho_m^-$). These dislocation densities are related to the strain rate via the Orowan relation:

$$\dot{\varepsilon} = b\rho_m v_g \tag{31}$$

where b is the length of Burgers vector, ρ_m the total mobile dislocation density and v_g the glide velocity in the primary slip plane. Moreover, the dislocation densities are related to the internal stress by the relation :

$$\sigma_i = \frac{\mu b}{2\pi\lambda} + \xi\mu b\sqrt{\rho_s} \tag{32}$$

with μ is the shear modulus and ξ is a constant. In the last equation the first contribution comes from obstacles such as precipitates or pre-existing walls separated by an effective spacing λ and, the second part is the contribution from the static dislocation population which also opposes

dislocation motion. The internal stress, σ_i, reduces the effective stress, σ_e, acting on the dislocations and where this last is defined as:

$$\sigma_e = \sigma_a - \sigma_i \tag{33}$$

with σ_a representing the applied stress. Finally, the glide velocity is related to the effective stress via appropriate phenomenological relations expressing the fact that individual dislocation motion is initiated when the effective stress acting on a dislocation exceeds the yield stress. This, for example, can be written as:

$$v_g \propto (\frac{\sigma_e}{\sigma_0})^m \tag{34}$$

or

$$v_g = v_0 \ \exp\left\{ -\frac{\mu}{kT}(\frac{\sigma_e}{\sigma_0})^{-m} \right\} \tag{35}$$

where σ_0 is the yield stress and $m > 1$. The essential features of the dislocation dynamics are, on the one side, their mobility, dominated by plastic flow, but which also includes thermal diffusion and climb, and, on the other side, the mutual interaction processes.

The essential features of dislocation dynamics are; their mobility , dominated by plastic flow which includes thermal diffusion and climb, and the mutual interaction processes. By taking into account these mechanisms, the resulting dynamical system can be written as (32):

$$\begin{aligned}
\partial_t \rho_s &= -\vec{\nabla} J_s + v_g \rho_m) \sqrt{\rho_s} - v_s d \rho_s^2 \\
&- v_g \delta \rho_m \rho_s - \beta \rho_s + v_g G(\rho_s) \rho_m \\
\partial_t \rho_m^+ &= -\vec{\nabla} \vec{J}_+ + \frac{\beta}{2} \rho_s - v_g G(\rho_s) \rho_m^+ - v_g \delta \rho_m^+ (\rho_s + \rho_m^-) \\
\partial_t \rho_m^- &= -\vec{\nabla} \vec{J}_- \frac{\beta}{2} \rho_s - v_g G(\rho_s) \rho_m^- - v_g \delta \rho_m^- (\rho_s + \rho_m^+)
\end{aligned} \tag{36}$$

where δ is the characteristic separation length between dislocations for spontaneous annihilation (114), d is the characteristic length of spontaneous dipole collapse, β is the frequency of dislocation freeing from the forest and is proportional to $v_g/\overline{d}$ where $\overline{d}$ is the characteristic dipole de-stabilization length which is inversely proportional to the effective stress, and $\beta = \beta_0 v_g \sigma_e$. The different characteristic lengths introduced here, or at least their order of magnitude, may in principle be evaluated from microscopic analysis (113; 114). Due to mutual interactions, thermal activation and climb, forest dislocations mobility is represented by a diffusive current $J = -D_s \vec{\nabla} \rho_s$, which represents the effective diffusion within the forest. The current of mobile dislocations is taken as $\vec{J}_\pm = \pm v_g \rho_m^\pm$ and represents the flux caused by gliding dislocations, in the present case, it is the flux caused by their edge component. Stability and numerical analyses of the previous set of equations have provided information on the conditions for formation of PSB's in fatigued specimens. It is shown that PSB formation is triggered by the clustering of dislocations or dislocation dipoles, which become finally immobile and arrange themselves in regularly spaced walls of high dislocation density (32).

Another statistical dynamical description has been proposed by Kratochvil et al. for the first stages of PSB formation. It is based on the evolution of dipolar loops, triggered by their interaction with gliding dislocations (115; 116; 117). The proposed statistical model is of the reaction-transport type, and focuses on the feedback between the evolution of glide velocity and the dipole density. The result is the sweeping of dipole loops by screw dislocations, which initiates the formation of dislocation walls. In this approach, dipole generation and interactions play a secondary role, and are introduced in an ad hoc and qualitative way.

In these proceedings, Thomson et al. (38) have also presented a new model for single crystal metal plasticity. Their proposed statistical approach rests on the fundamental observations that deformation is characterized by partially ordered internal dislocation wall structures, discontinuous strain bursts in time, and strain localization in a surface slip band structure. A percolation strain model corresponding to elementary slip line burst events, with percolation parameters to be supplied from experiments and dislocation dynamics studies of wall structures, was developed. They proposed a model for localization of the slip lines into bands, which envisions channels for slip formed from the dense planar walls. Their continuum model is based on two different material properties in the slip bands, and in the matrix between the bands.

3 A Brief Outline of Current Topics

In this symposium, 23 presentations were given on subjects covering the entire range of models within the multi-scale materials modeling framework. The articles following this review paper are representatives of state-of-the art theoretical and experimental methodologies to adress the mechanics of materials at the nano- and micro-scale. These are classified into atomistic, mesoscopic and continuum models. In the following, we give a brief introduction of the topics covered by these papers.

3.1 Atomistic Models

Five articles are focused on atomistic modelling of defect structures in solids. Microscopic defects play critical role in determining materials response to external stresses beyond elastic response, and have intrinsic atomic structures. Therefore, atomistic modelling is crucial to elucidate the detailed mechanisms operating during the materials responses.

Wei et al. (118) presented MD simulation study of carbon nanotube mechanics under uniaxial compression, and this work illustrates the capability of atomistic simulations in nanomechanics research. In this work, Tersoff-Brenner bond-order potential is used to accurately describe chemical bond breaking and formation processes in carbon nanotubes. The authors have focused their simulation work on the plastic response of carbon nanotubes under large strain beyond the yield strength. To find realistic mechanisms, temperature acceleration techniques has been used to overcome energy barriers and to escape from local minimum energy configurations. It is shown that at T = 0 the nanotube under 12% compressive strain does not have plastic response confirming previous findings of other MD simulations. The authors have systematically increased the temperature T = 300, 800, 1200, and 1600 K to investigate the temperature effects and found that there are two distinct plasticity mechanisms: diamond-like tetrahedral bond formation, and dislocation pair formation (also known as Stone-Wales defect). This work has confirmed the importance of the time scale problem in atomistic simulations since high temperature simulation with high strain rate would have similar effects as low temperature simulation with low strain rate.

Li and Yip (119) have reviewed the atomistic simulations to determine material strength based on the key-note talk given by S. Yip at the Symposium. In this paper, mechanical stability criteria of elastic materials are reviewed and applied to study SiC crystal under hydrostatic tension and Cu thin film under indentation. For cubic SiC in 3C or β-phase, phonon dispersion curves are examined under hydrostatic tension and pure shear to elucidate the relationship between stability criteria and phonon softening. The authors have studied the yield strength of SiC perfect crystal, nanocrystal, and amorphous solid and found that the nanoscale grain size and atomic scale defects determine the ultimate tensile strenght of solids. Their findings are summarized in scaling behavior of cross over from Hall-Petch relation at large grain sizes to nanograins down to amorphous solids. Using hard nanoindentor on Cu(111) surface, the authors have found that the plastic response of the thin film proceeds through intermittent plasticity in which burst of dislocations are emitted below the indentor. Finally, the authors have provided an outlook on the role of multiscale simulations for materials strength.

Atomistic simulation method is applied to investigate dislocation nucleation mechanisms of W thin film during the deposition process by Liu et al. (120). In this owrk, the authors have used Finnis-Sinclair form potential to W($1\bar{1}0$) thin films under growth condition of adding W atoms with 0.01 eV kinetic energy. Uniaxial tensile stress of 13 GPa is applied along [111] direction to simulate the substrate-film mismatch effects. Detailed investigations performed with a very high temperature (2500 K) to accelerate the kinetic processes in MD time scale. From the simulations, it is discovered that the dislocation nucleation initiates at the surface steps and as a consequence the sharp surface step has been removed to reduce the surface strain through dislocation motion.

Lin and Chrzan (121) have also investigated the dislocation using atomistic simulations. The authors have focused the investigation on the core structure and energetics of 90° partial dislocation in Si crystal. Tersoff potential is used to determine the optimized atomic configuration and energy of the dislocation under hydrostatic stresses. A detailed analysis is performed for two different core structure of the dislocation: single-period (SP) reconstruction and double-period (DP) reconstruction. The authors have used periodic boundary condition for an infinite array of dislocations and the periodic interaction effects are compensated through continuum elastic analysis. The accuracy of this analysis is tested using cylindrical boundary condition with increasing radius up

to 70Åand a good agreement was obtained confirming validity of the use of periodic boundary condition. At zero external stress DP core reconstruction is found to be more stable by 7 meV/Å, but it is also found that shear stress reduce the relative stability of DP compared to SP reconstructions. When hydrostatic pressure is applied to Si crystal the energy difference is further reduced leading to a stress induced phase transition of dislocation core structure from DP to SP reconstructions. This core structure transition may paly an important role in dislocation kinetics.

Kuramoto et al. (122) have investigate the interactions between point defects (interstitial atoms and vacancies) and microstructures (dislocations, interstitial clusters, and stacking fault tetrahedrons) using EAM-type potentials for BCC Fe and FCC Ni crystals. The authors have performed detailed energetics study of the interactions between point defects and microstructures leading to capture zone analysis at 500°C. It is found that the self interstitial atoms (crowdions and bumbbells) have large capture zone than vacancies for edge dislocation in Fe and Ni. Capture zones of self interstitial atoms by interstitial clusters are smaller than those of edge dislocations for Fe. The capture zones of stacking fault tetrahedrons are larger for interstials than vacancies in Ni crystal. The overall energetics elucidates the origin of preferential removal of interstitials during the evolution of damage structures in irradiated meterials. The microstructures capture the interstitial defects and leave excess vacancies. These vacancies nucleate during subsequent evolution leading to void foramtion and swelling of irradiated materials.

3.2 Mesoscopic Models

Three contributed articles to these proceedings have addressed aspects of mesoscopic plastic deformation, from the theoretical (38), computational (123) and experimental (124) points of view. Thomson et al.(38) presented a multiscale theoretical framework for metal plasticity of single crystals. Their approach is based on the experimental observations that deformation is characterized by partially ordered internal dislocation wall structures, discontinuous strain bursts in time, and strain localization in a surface slip band structure. The main approach follows a statistical percolation strain model, whic corresponds to elementary slip line burst events. Phenomenological percolation parameters in their model are to be supplied from experiments and dislocation dynamics studies of wall structures. A model for localization of the slip lines into bands is proposed, which envisions channels for slip formed from the dense planar walls. This is suplemented by a continuum model that is constructed from the outputs of the percolation model. The continuum model has two principal internal variables, and exhibits the desired hardening behavior with strain. The continuum model is based on two different material properties in the slip bands, and in the matrix between the bands. Althou thier analysis does not include dislocation patterning mechanisms, it addresses the transport of dislocations through these structures.

The work of Martinez and Ghoniem (123) focuses on the direct coupling of Dislocation Dynamics (DD) with the Finite Element Method (FEM) to simulate plastic deformation of micro-scale structures. They attempt to address the in effects of crystal surfaces on dislocation motion. Three-dimensional DD simulations of BCC single crystals with a single shear loop in the (101)-[111] slip system are performed to explore the relationship between loop force distributions and the proximity of the loop to the crystal boundaries. Traction boundary conditions on a single crystal model are satisfied through the superposition of a complementary stress field computed by the FEM, and the elastic stress field of dislocations computed by DD. The deformation and expansion of dislocation loops is computed using a Galerkin variational energy method, and the equilibrium geometry is determined. The deformation of a Frank-Reed (FR)source in a single crystal model is also determined in their computer simulations. Their results indicate that crystal surface forces play a significant role in dislocation force distributions and deformation to a depth from the surface, which is proportional to the loop radius. Large out-of-plane force distributions on closed loops on oblique slip plane/free surface orientations are shown. These forces act in such a way as to repel loop motion from the intersection of the slip plane with the free surface, while causing deformation through the mechanism of cross-slip. Expansion or contraction of shear loops is found to be dependent on the critical applied stress, the radius of curvature, and the proximity and orientation of the loop with respect to the crystal surface.

Experimental work that is directed towards verification of dislocation dynamics models has been presented by Hsuing and Lassila (124). In this work, the initial dislo-

cation microstructure in as-annealed high-purity Mo single crystals, and the deformation substructures of crystals compressed at room temperature at different strain rates were examined. The main objective of this work is to determine the physical mechanisms of dislocation multiplication and motion during the early stages of plastic deformation. The initial dislocation density was measured to be in a range of $10^6 \sim 10^7\ cm^{-2}$. Numerous grown-in superjogs were observed along screw dislocation lines. After testing in compression, dislocation density (mainly screw dislocations) increased to $10^7 \sim 10^8\ cm^{-2}$. The formation of dislocation dipoles as a result of the nonconservative motion of jogged screw dislocations was found to be dependent on the strain rate. At low strain rates (e.g. $\dot{\varepsilon} \sim 10^{-3}\ s^{-1}$) small concentrations of dislocation dipoles were found in crystals. However, more cusps along screw dislocation lines and numerous dislocation dipoles were observed in crystals compressed at strain rates of $1\ s^{-1}$.

3.3 Continuum Models

Two papers in these proceedings have been concerned with applications of continuum mechanics to multiscale material problems, particularly to represent fracture processes (125), and surface laws during slip (126) . The recently developed virtual-internal-bond (VIB) model has incorporated a cohesive-type law into constitutive lequations, such that fracture and failure are embedded into the constitutive law, and no separate failure criteria is needed. Zhang et al. developed a numerical algorithm for the VIB model under static loadings. The model is applied to study three examples: (1)crack nucleation and propagation from a stress concentration site; (2) kinking and subsequent propagation of a mode II crack, and (3) buckling-driven delamination of a thin film from its substrate. Their results have shwon that the VIB model provides an effective method for studying crack nucleation and propagation in engineering materials.

In another paper on continuum mechanics, the embedding of micromechanical models in the macromechanical formulation was treated by a variational multiscale method (126). A scale separation is introduced on the displacement field into coarse and finne scale components. The fine scale displacement is governed by the desired micromechanical model, and is eliminated by expressing it in terms of the coarse scale displacement and the remaining fields in the problem. The resulting macromechanical formulation is posed solely in terms of the coarse scale displacements, but is influenced by the fine scale; thereby it has a multiscale character. The procedure results in an embedding of the micromechanical model in the macromechanical formulation. Garikapati applied this general approach to the special case of traction-displacement laws on internal surfaces. Numerical examples were presented that demonstrate the method for several benchmark problems.

4 Current Challenges

The field of Multiscale modeling of materials is perhaps not new or even novel! Since the early days of modern physics, scientists have attempted to develop simple mathematical relations that can reduce the enormous number of degrees of freedom (DOF) in a given system to its bare minimum. In fact, this approach is quite consistent with our desire to reduce the number of observables to what can be realistically perceived. The magic of statistical mechanics, for example, lies in the fact that the collective behavior of atoms of infinite degrees of freedom can be described by simple scaling laws. This trend stems from the fact that *averaging* works very well, when things are away from *catastrophes*! Thus, most of the relevant information in cosntitutive equations represent some averaged behavior of many, many atoms. However, when one examines material systems at the nano- and micro-scale, many of these concepts start to present a real challenge. As we discussed before, the law of large numbers, which is central in statistical mechanics, does not hold in situations where we do not have adequate sampling phase space. In the mean-time, phase transitions, nucleation, plasticity, and fracture are all critical phenomena that represent material *catastrophes*, and hence averaging techniques will not yield the correct information.

Nevertheless, the advent of large-scale computing is propelling the art and science of modeling material phenomena into a tantalizing new direction. Instead of attempting to reduce the complexity of the material system's behavior by a process of reduction of its DOF, one is trying to represent large numbers of DOFs, and solve for them numerically! The result is a real numerical experiment, whose outcome is not known *a priori*. Whether that makes sense can only be tested by confronting the outcomes of computer simulations with a limited range of experimental observations. Over a decade ago, such a process has been viewed with great skepticism. In part,

this skepticism stems from the realization that computer simulations are also based on some *ad hoc* assumptions, and that the numerics still represent gross approximations. However, the last decade has seen tremendous advances on a number of computational and physical fronts that have alleviated most of that skepticism. Adavancs have been made in atomistic simulation techniques, with better and more rigorous ways to approximate the quantum mechanical behavior of atoms and molecules. These advances have been matched by the ability to devise empirical, yet physically-based interatomic potentials for performing more accurate classical MD simulations. The simulated system size has also increased, almost exponentially, during the past decade, thanks to the increase in computing power and reduction in its cost. The connection between classical MD and ab intio calculations are now being made in a clear and rigorous fashion.

At the meso-scale, inbetween the atomistic and macroscopic, a few attempts have made it possible to find new in-roads into modeling this forbidding regime! Over a decade ago, there were only 2-D computer simulations of collective dislocation phenomena. The confidence in the realism of these simulations was not very high, because several ad hoc rules had to be introduced to account for short-range dislocation processes. Nonetheless, the fact that several phenomena of dislocation pattern formation were demosnstrated with direct computer simulations gave rise to hope that there is something useful to be done in this area. Recently, reserach on mesoscopic plsticity models has kicked into high gears, as a result of concentrated efforts by many groups around the world to develop a physical description of plastic deformation. These efforts utilize new computational methods of 3-D Dislocation Dynamics, as well as new physical statistical models for the collective behavior of dislocations.

Although it is felt now that sooner or later, a coherent description for the mechanics of materials will emerge, and that such a description will be physically-based with no ad hoc assumptions, the road is still not entirely clear. A number of challenges and obstacles remain, as we briefly discuss them in the following. The main challenges in the development of *seamless* multi-scale modeling methodology are the length-scale, the time-scale, the numerical accuracy and the self-consistency of multiscale models, as outlined below.

4.1 The Length Scale

The number of atomic degrees of freedom in a typical material system is extremely large, and if one is to model a cubic micron of the material, the equations of motion of a few billion atoms must be numerically solved. At the sub-continuum length scale, the material system of interest is usually small enough that current computing capabilities can model it realistically. Furthermore, there exist several multiscale methods to combine atomistic model and continuum models in a single simulation framework. These atomistic and multiscale methods have been successfully applied to investigate diverse defect structures within static or quasi-static descriptions.

Even though some aspects of the length scale problem have been overcome in the sense that one can model the material system of interest with full atomic scale details, there remains the very challenging problem of structural complexity at meso-scales. As the number of atoms in a system increases, the possible local minimum energy configurations also grow very rapidly. Analysis of N atom cluster shows that the number of local minimum energy configurations grows faster than e^N. Without knowing all the relative energy values of these local configurations, it is very difficult to prepare initial atomic configurations which are most relevant to real physical systems. This problem of configuration multiplicity is closely related to the other problems of time scale and accuracy of atomistic simulations. If one can run simulations long enough for a system to search through all the relevant configurations, the complexity of the atomic structures can be overcome by systematic sampling with different initial configurations. On the other hand, the inaccuracy of an interatomic potential can introduce errors in relative energies of diverse configurations and also in energy barriers separating different configurations. Both of these problems seriously influence the reliability of atomistic simulations.

Although substantial recent progress has been made in the mesoscopic simulation area, a number of challenges remain. As the system size becomes within the nano- and micro-scale, applications of 3-D DD becomes very attractive. The number of dislocation loops required to represent full-scale plasticity of a sub-micron crystal is relatively manageable, and the solution requires integration of a few thousand equations of motion. However, the long-range nature of the stress field of dislocations, the topological complexity of dislocation lines, the treat-

ment of periodic boundary conditions that ensure statistical consistency of the results, the accurate solution of dislocation interaction with surfaces and the inclusion of elastic anisotropy and inertial effects into dislocation dynamics remain as tough, yet doable problems in the near future. The more challenging problem of polycrystalline plasticity will require additional breakthroughs, because of the conceptual difficulties of connecting DD to crystal plasticity models in a self-consistent fashion. The main question here is how to retain the characteristic length scale from the discrete dislocation to the continuum description. A variety of strain gradient theories have been proposed during the last decade. Since most of them are formulated in a phenomenological manner, the characteristic length scale in invoked into the theory, without rigorous treatment of its dislocation origins. In addition, there are indications that a single length scale is not always realistic, and that a spectrum of scales may be more appropriate. These issues will require intensive research to clearly establish the links between mesoscopic simulations and continuum mechanics.

4.2 The Time Scale

The severe limitaions on the total simulation time in atomistic modeling is a result of the intrinsic time scale of atomic dynamics, which is typically on the order of femto seconds. In numerical simulations using finite time steps, the step size is required to be small enough to keep the numerical simulation stable. Sub-continuum microstructure evolution is not an equilibrium process, and there are complex defect structural changes during kinetic processes. Therefore, it is necessary to follow the dynamic evolution of a system over a realistic experimental time scale to accurately describe microstructure evolution mechanisms. The experimental time scales are very long (micro seconds or larger), compared to atomic time scales so that more than billion time steps are needed for these simulations.

Diverse simulation techniques are currently developed to overcome this time scale problem. These efforts are based on the observation that while the atomic time scale is determined by thermal motion of atoms around a local minimum energy configuration, the kinetic evolution of the microstructure is dictated by much slower transitions between neighboring local minimum configurations. Kinetic Monte Carlo (KMC) is a popular method to overcome the atomic time scale problem by evolving the system directly from one configuration to another configuration without thermal motion of atoms. However, KMC requires a complete list of possible events to simulate the time evolution of a system, and this list is known as the event catalogue. The accuracy of KMC is critically governed by the accuracy and completeness of the event catalogue. If a critical event is missing in the catalogue, the resulting KMC evolution may not provide meaningful information of the simulated system. The same argument applies to the accuracy of the transition rates in the event catalogue.

Another approach to overcome the time scale limitations in atomistic simulations is to modify the MD scheme in such a way that the duration of thermal motion is shortened, or that the configuration search is accelerated. Several promising methods (e.g., hyperdynamics) are currently developed, but the general applicability of these new methods to complex atomic processes is yet to be firmly established. Another promising direction is to develop a systematic scheme to search possible events using accelerated MD methods or direct configuration space search methods. Nudged elastic band (NEB) is such a method which can be used to identify transition states separating initial and final configurations. This systematic search of events will enable a systematic development of event catalogues for KMC simulations.

When one considers the evolution of the dislocation microstructure, similar imitations are immediately obvious. When two dislocations interact at close range, such as the case for junction or dipole formation, the dynamics is very fast, with time steps on the order of picoseconds. On the other hand, the evolution of dislocation cell walls and persistent slip bands occurs on a much longer time scale, on the order of kiloseconds, characteristic of fatigue and creep processes. These transitions from direct DD simulations (which are in fact for very short time scales) to longer time scales characteristic of experimental observations remain as a challenge.

4.3 Accuracy

The accuracy of interatomic potentials in classical atomistic simulations (MD, MC, KMC) is a critical problem since interatomic potentials are reliable only within the range of parameter fitting. Therefore, the question of the influence of the accuracy of empirical interatomic potentials on the predictions of atomic simulations of large systems is vexing, and casts doubts on the fidelity of fi-

nal conclusions. The accuracy problem can be overcome by quantum simulation, but the stiff increase in computational cost associated with quantum simulations limits its applicability to very small nano-scale systems. Since the accuracy problem of interatomic potentials is intrinsic to classical atomistic simulations, it is necessary to understand the range of validity of each interatomic potential. Based on a clear understanding of the limitations and accuracy of interatomic potentials, it will be possible to extract reliable conclusions from atomistic simulations.

Mesoscopic simulations have also been confronted with severe accuracy issues during this past decade. At the lowest level of desired accuracy, dislocations can be discretized into relatively long segments with average Peach-Koehler forces acting on them, and with crude estimates of the self forces retraining them. Several methods, as discussed earlier, have emerged to engender higher levels of accuracy and rigor to these earlier treatments. In this regard, benchmark problems have been used to gauge the accuracy of simulations, with added rigor to the underlying theory. However, when one considers fully-anisotropic materials, or in truly dynamical applications such as high-speed deformation, the computational cost increases by several orders of magnitude to achieve the same level of accuracy. It is expected, therefore, that a variety of levels of approximations will be applicable for the solution of specific problems, and that in some cases, a rigorous treatment would be an over-kill, while in others, it may not give accurate information. The challenge here is to identify where and how to apply the various levels of approximations with mesoscopic simulations.

4.4 Self-consistency of Multi-scale Models

At the present time, there appears to be a great need to develop general mathematical and computational methods for a truly *seamless multiscale* approach to computer simulations of nano- and micro-systems. Since the field is in its infancy, the computational techniques are developed within a specified range of space and time scales. There seems to be the understanding that the transition between one space-time range to another is carried out by a process of *hand-shaking*, that is the information gained from a lower scale is summarized into a finite set of parameters, and passed on to the higher scale. This procedure is acceptable, as long as such parameters are well-defined, and represent a rigorous reduction of the enormous degrees of freedom of a lower length scale into a few generalized degrees of freedom represented by those parameters. However, theoretical foundations and computational implementation of a more rigorous process remain unresolved. If there could be generlizations of the concept of degress of freedom from those associated with space-time (e.g. geometry), to those representative of statistical configurations (e.g. conductivity, mobility, etc.), then smooth transitions between various length scales can be worked out.

5 Future Directions

Multiscale Modeling of Materials (M^3) is in its very early stage of development, and there are many scientific and mathematical problems to be addressed in the future. It is a rich field of physical, numerical, computational, and mathematical challenges. It is also going to play a key role in the simulation and design methodology for the newly emerging field of nanotechnology. The practical application of multiscale simulation will be in the analysis and design of nano- and micro-scale devices, and we expect that the next decade will be critical for this development. There are many exciting engineering science problems as well as practical nano- and micro-device applications waiting for us to investigate with M^3. The key problems to be investigated in the future are: (1) the limitations on the time scale in atomistic and mesoscopic simulations, (2) the limitaions on the length scale in atomistic and mesoscopic simulations, (3) the effects of modeling accuracy on the simulation results, and (4) the development of self-consistent seamless methods of multi-scale.

Acknowledgments

Research is supported by the US Department of Energy, Office of Fusion Energy, through Grant DE-FG03-00ER54594, and the National Science Foundation (NSF) through grant DMR-0113555 with UCLA, and the US Department of Energy, through Grant DOE PG03-99ER45788, and the National Science Foundation (NSF) through Grant NSF EEC-0085569, with Stanford University. Contributions of Mr. Ming Wen to the KMC discussion are appreciated.

References

[1]**Peng, S.; Cho, K.** (in press, 2002): Nano Electro

Mechanics of Semiconducting Carbon Nanotube. *J. Appl. Mech.*

[2]**Amodeo, R. J.; Ghoniem, N. M.** (1988): A Review of Experimental Observations and Theoretical Models of Dislocation Cells and Subgrains. *Res Mechanica*, vol. 23, pp.137-160.

[3]**Mughrabi, H.** (1987): A 2-parameter Description of Heterogeneous Dislocation Distributions in Deformed Metal Crystals. *Material Science and Engeering*, vol. 85, pp. 15-31.

[4]**Mughrabi, H.** (1983): Dislocation Wall and Cell Structures and Long-range Internal-stresses in Deformed Metal Crystals. *Acta Mettalurgica*, vol. 31, (n. 9), pp. 1367-1379.

[5]**Lepinoux, J.; Kubin, L. P.** (1987): The dynamic organization of dislocation structures: a simulation. *Scripta Met.*, vol. 21, pp. 833-838.

[6]**Ghoniem, N. M.; Amodeo, R.** (1988): Computer Simulation of Dislocation Pattern Formation. *Solid State Phenomena*, vol. 3&4, pp. 377-388.

[7]**Amodeo, R. J.; Ghoniem, N. M.** (1988): Dynamical Computer Simulation of the Evolution of a One-Dimensional Dislocation Pileup. *International Journal of Engineering Science*, vol. 26, pp. 653-662.

[8]**Ghoniem, N. M.; Amodeo, R. J.** (1990): Numerical simulation of dislocation patterns during plastic deformation. In *Patterns, Defects and Material Instabilities*, Eds. D. Walgreaf and N. M. Ghoniem, Kluwer Academic Publishers, Dordrecht, pp. 303.

[9]**Amodeo, R. J.; Ghoniem, N. M.** (1990): Dislocation Dynamics: Part I-A Proposed Methodology for Deformation Micromechanics. *Phys. Rev. B*, vol. 41, pp. 6958-6967.

[10]**Amodeo, R. J.; Ghoniem, N. M.** (1990): Dislocation Dynamics: Part II-Applications to the Formation of Persistent Slip Bands, Planar Arrays, and Dislocation Cells. *Physics Review B*, vol. 41, pp. 6968-6976.

[11]**Amodeo, R. J.; Ghoniem, N. M.** (1991): Rapid Algorithms for Dislocation of Dynamics in Micro mechanical Calculations. In *Modeling of Deformation of Crystalline Solids*, Eds. T. Lowe, T. Rollett, P. Follansbee, and G. Daehn, TMS Press, pp. 125.

[12]**Ghoniem, N. M.** (1992): Non-Linear Dynamics of Shear Crack Interaction with Dislocations. In *Non-Linear Phenomena in Material Science II*, Eds. L. Kubin and G. Martin, Kluwer Academic Publishers.

[13]**Guluoglu, A. N.; Srolovitz, D. J.; LeSar, R.; Lomdahl, R. S.** (1989): Dislocation Distributions in Two Dimensions. *Scripta Metallurgica*, vol. 23, (no. 8), pp.1347-1352.

[14]**Groma, I.; Pawley, G. S.** (1993): Computer Simulation of Plastic Behaviour of Single Crystals. *Philosophical Magazine A (Physics of Condensed Matter, Defects and Mechanical Properties)*, vol. 67, (no. 6), pp.1459-1470.

[15]**Lubarda, V. A.; Blume, J. A.; Needleman, A.** (1993): An Analysis of Equilibrium Dislocation Distributions. *Acta Metallurgica et Materialia*, vol. 41, (no. 2), pp. 625-642.

[16]**Elazab, A.; Ghoniem, N. M.** (1993): Green's Function for the Elastic Field of an Edge Dislocation in a Finite Anisotropic Medium. *International Journnal of Fracture Mechanics*, vol, 61, pp. 17-37.

[17]**Wang, H. Y.; LeSar, R.** (1995): O(N) Algorithm for Dislocation Dynamics. *Philosophical Magazine A (Physics of Condensed Matter, Defects and Mechanical Properties)*, vol. 71, (no. 1), pp.149-64.

[18]**Kubin, L. P.; Canova, G.; Condat, M.; Devincre, B.; Pontikis, V.; Brechet, Y.** (1992): Dislocation Microstructures and Plastic Flow: a 3D Simulation. *Diffusion and Defect Data - Solid State Data, Part B (Solid State Phenomena)*, vol. 23-24, pp. 455-72.

[19]**DeVincre, B.; Condat,M.** (1992) *Acta Met. Mater.*, vol. 40, pp. 2629.

[20]**DeVincre,B.; Pontikis, V.; Brechet,Y.; Canova, G.; Condat, M.; Kubin, L. P.** (1992): Three-dimensional Simulations of Plastic Flow in Crystals. in *Microscopic Simulations of Complex Hydrodynamic Phenomena*, Ed. M. Mareschal and B. L. Lolian, Plenum Press, New York, pp. 413-423.

[21]**Canova, G.; Brechet, Y.; Kubin, L. P.** (1992): 3D Dislocation Simulation of Plastic Instabilities by Work-softening in Alloys. In *Modeling of Plastic Deformation and its Engineering Applications*,

Eds. S. I. Anderson et al., RIS∅ National Laboratory, Roskilde, Denmark.

[22]**Kubin, L. P.; Canova, G.** (1992): The Modelling of Dislocation Patterns. *Scripta Metallurgica et Materialia*, vol. 27, (no. 8), pp. 957-62.

[23]**Kubin, L. P.** (1993): Dislocation Patterning during Multiple Slip of FCC Crystals. A simulation Approach. *Physica Status Solidi A*, vol. 135, (no. 2), pp. 433-443

[24]**Canova G.; Brechet Y.; Kubin, L. P.; DeVincre, B.; Pontikis, V.; Condat, M.** (1994): 3D Simulation of Dislocation Motion on a Lattice: Application to the Yield Surface of Single Crystals. *Microstructures and Physical Properties*, Ed J Rabiet, **CH-Transtech**.

[25]**Devincre, B.; Kubin, L. P.** (1994): Simulations of Forest Interactions and Strain Hardening in FCC Crystals. *Modelling and Simulation in Materials Science and Engineering*, vol. 2, (no. 3A), pp. 559-570.

[26]**Hirth, J. P.; Rhee, M.; Zbib, H.** (1996): Modeling of Deformation by a 3D Simulation of Multi Pole, Curved Dislocations. *Journal of Computer-Aided Material Design*, vol. 3, pp. 164.

[27]**Zbib, R. M.; Rhee, M.; Hirth, J. P.** (1998): On Plastic Deformation and the Dynamics of 3D Dislocations. *International Journal of Mechanical Sciences*, vol. 40, (no. 2-3), pp. 113-127

[28]**Rhee, M.; Zbib, H. M.; Hirth, J. P.; Huang, H.; de la Rubia, T.** (1998): Models for Long-/short-range Interactions and Cross Slip in 3D Dislocation Simulation of BCC Single Crystals. *Modelling and Simulation in Materials Science and Engineering*, vol. 6, (no. 4), pp. 467-492.

[29]**Schwarz, K. V.; Tersoff, J.** (1996): Interaction of Threading and Misfit Dislocations in a Strained Epitaxial Layer. *Applied Physics Letters*, vol. 69, (no. 9), pp.1220-1222.

[30]**Schwarz, K. W.** (1997): Interaction of Dislocations on Crossed Glide Planes in a Strained Epitaxial Layer. *Physical Review Letters*, vol. 78, (no. 25), pp. 4785-4788.

[31]**Schwarz, K. W.; LeGoues, F. K.** (1997): Dislocation Patterns in Strained Layers from Sources on Parallel Glide Planes. *Physical Review Letters*, vol. 79, (no. 10), pp.1877-1880.

[32]**Walgraef, D.; Aifantis, C.** (1985): On the Formation and Stability of Dislocation Patterns. I. One-dimensional Considerations. **International Journal of Engineering Science**, vol. 23, (no. 12), pp. 1351-1358.

[33]**Hähner, P.; Bay, K.; Zaiser, M.** (1998): Fractal Dislocation Patterning During Plastic Deformation. *Physical Review Letters*, vol. 81, (no. 12), pp. 2470-2473.

[34]**Hähner, P.** (1996): *Appl. Phys. A*, vol. 62, 473.

[35]**Zaiser, M.; Hähner, P.** (1997): Oscillatory Modes of Plastic Deformation: Theoretical Concepts. *Physica Status Solidi B*, vol. 199, (no. 2), pp. 267-330.

[36]**Zaiser, M.; Avlonitis, M.; Aifantis, E. C.** (1998): Stochastic and Deterministic Aspects of Strain Localization During Cyclic Plastic Deformation. *Acta Materialia*, vol. 46, (no. 12), pp. 4143-4151

[37]**El-Azab, A.** (2000): *P*hys. Rev. B, vol. 61, pp. 11956.

[38]**Robb Thomson, L. E. Levine, Y. Shim, M. F. Savage, and D. E. Kramer**: A Multi-Scale Theoretical Scheme for Metal Deformation. These Proceedings.

[39]**Ziman, J.M.** (1972): Principles of the Theory of Solids.

[40]**Car, R.; Parrinello, M.** (1985),"Unified Approach for Molecular Dynamics and Density Functional Theory," *Phys. Rev. Lett.*, vol. 55, pp. 2471-2474.

[41]**Srivastava, D.; Menon, M.; Cho, K.** (2001): Computational Nanotechnology with Carbon Nanotubes and Fullerenes. *Computing in Science & Engineering*, vol. 3, pp. 42-55.

[42]**Payne, M. et al.** (1992): Iterative minimization techniques for ab initio total-energy calculations: molecular dynamics and conjugate gradients. *Rev. Mod. Phys.* vol. 68, pp. 1045-1097.

[43]**Hohenberg, P.; Kohn, W.** (1964): *Phys. Rev.* vol. 136, pp. 864B.

[44]**Kohn, W.; Sham, L.J.** (1965): *Phys. Rev.* vol. 140, pp. 1133A.

[45]Ab intio Simulation Package (VASP)at the web site http://cms.mpi.univie.ac.at/vasp/.

[46]ABINIT code at the web site http://www.mapr.ucl.ac.be/ABINIT/.

[47]DFT++ Computer Code at http://elrio.mit.edu/dft++/.

[48]Molecular Simulation software at http://www.accelrys.com/about/msi.html.

[49]**Kawamoto, A.; Jameson, J.; Cho, K.; Dutton, R.W.** (2000): Challenges for Atomic Scale Modeling in Alterantive Gate Stack Engineering. *IEEE Trans. Electro. Dev.*, vol. 47, pp. 1787-1794.

[50]**Daw, M.; and Baskes, M.** (1983) *Phys. Rev. Lett.* vol. 50, pp. 1285.

[51]**Daw, M.; and Baskes, M.** (1984) *Phys. Rev. B* vol. 29, pp. 6443.

[52]**Pearson, E.; Takai, T.; Halicioglu, T.; and Tiller, W.** (1984) *J. Cryst. Growth*, vol 70, pp. 33.

[53]**Stillinger, F.; and Weber, T.** (1985) *Phys. Rev. B.*, vol. 31, pp. 5262.

[54]**Tersoff, J.**, (1986) *Phys. Rev. Lett.*, vol. 56, pp. 632.

[55]**Gear,C. W.** (1971): *N*umerical Initial Value Problems in Ordinary Differential Equations, Prentice-Hall, Englewood Cliffs, N.J.

[56]**Rapaport, D. C.** (1995): *The Art of Molecular Dynamics Simulation*, Cambridge University Press.

[57]**Frenkel, D.; Smit, B.** (1996): *Understanding Molecular Simulation*, Academic Press.

[58]**Haile, J. M.** (1992): *Molecular Dynamics Simulation*, Wiley Interscience.

[59]**Wang, Jian; Woo, C. H.; Huang, Hanchen** (2001): Destabilization of Dislocation Dipole at High Velocity. *J. Appl. Phys. Lett.*, **79(22)**, 101.

[60]**Nyberg A.; Schlick, T.** (1991): *J. Chem. Phys.*, vol. 95, pp. 4989.

[61]**James, F.** (1990): A Review of Pseudorandom Number Generators. *Computer Physics Communications*, vol. 60, (n. 3), pp. 329-344.

[62]**James, F.** (1980): Monte Carlo Theory and Practice. *Reports on Progress in Physics*, vol. 43, (n. 9), pp. 1145-1189.

[63]**Doran, D. G.** (1970): Computer Simulation of Displacement Spike Annealing. *Radiation Effects*, vol. 2, (n. 4), pp. 249-267.

[64]**Beeler, J. R.** (1982): *Radiation Effects Computer Experiments*. Amsterdam, Netherlands: North-Holland.

[65]**Heinisch, H. L.** (1995): Simulating the Production of Free Defects in Irradiated Metals. *Nuclear Instruments & Methods in Physics Research, Section B (Beam Interactions with Materials and Atoms)*, vol. 102, pp. 47-50.

[66]**Battaile, C. C.; Srolovitz, D. J.** (1997): A kinetic Monte Carlo Method for the Atomic-scale Simulation of Chemical Vapor Deposition: Application to Diamond. *Journal of Applied Physics*,vol. 82, (n. 12), pp.6293-6300.

[67]**Metropolis, N.; Rosenbluth, A. W.; Rosenbluth, M. N.; Teller, A. H.; Teller, E.** (1953): *Journal of Chemical Physics*, vol. 21, pp. 1087.

[68]**Bortz, A. B.; Kalos, M. H.; Lebowitz, J. L.** (1975) A New Algorithm for Monte Carlo Simulation of Ising Spin Systems. *Journal of Computational Physics*, vol. 17, (n. 1), pp.10-18.

[69]**Huang, Hanchen; Gilmer, G. H.; Diaz de la Rubia,T.** (1998): An Atomistic Simulator for Thin Film Deposition in Three Dimensions. *Journal of Applied Physics*, vol. 84, pp. 3636-3649.

[70]**Gilmer, G. H.; Huang, Hanchen; Diaz de la Rubia,T.; Torre, J. D.; Baumann, F.** (2000): Lattice Monte Carlo Models of Thin Film Deposition, an invited review. *Thin Solid Films*, vol. 365, pp. 189-200.

[71]**Wen, W.; Ghoniem, N. M.** (in preparation): Kinetic Monte Carlo computer simulations of Self-Interstitial Atom (SIA) cluster motion in stressed crystals.

[72]**Singh, B.; Foreman, A.J.E.; and Trinkaus, H.** (1997) *J. Nucl. Mater.*, vol 249, pp. 103.

[73]**Lepinoux,J.; Kubin, L. P.** (1987): The Dynamic Organization of Dislocation Structures: a Simulation. *Scripta Metallurgica*, vol. 21, (no. 6), pp.833-838.

[74]**Ghoniem, N. M.; Amodeo, R.** (1988): Computer simulation of dislocation pattern formation. *Solid State Phenomena*, vol. 3& 4, pp. 377-388.

[75]**Guluoglu, A. N.; Srolovitz, D. J.; LeSar R.; Lomdahl, R. S.** (1989): Dislocation distributions in two dimensions. *Scripta Metallurgica*, vol. 23, pp. 1347.

[76]**Amodeo, R. J.; Ghoniem, N. M.** (1990): Dislocation dynamics. I. A Proposed Methodology for Deformation Micromechanics. *Physical Review B (Condensed Matter)*, vol. 41, pp. 6958-6967.

[77]**Amodeo, R. J.; Ghoniem, N. M.** (1990): Dislocation dynamics. II. Applications to the Formation of Persistent Slip Bands, Planar Arrays, and Dislocation Cells. *Physical Review B (Condensed Matter)*, vol. 41, pp. 6968-6976.

[78]**Amodeo, R. J.; Ghoniem, N. M.** (1991): Rapid Algorithms for Dislocation of Dynamics in Micromechanical Calculations. in *Modeling of Deformation of Crystalline Solids*, Eds. T. Lowe, T. Rollett,P. Follansbee, and G. Daehn, TMS Press, pp. 125.

[79]**Groma I.; Pawley, G. S.** (1993): Computer Simulation of Plastic Behaviour of Single Crystals. *Philosophical Magazine A*, vol. 67, (no. 6), pp. 1459-1470.

[80]**Lubarda, V. A.; Blume, J. A.; Needleman, A.** (1993): An Analysis of Equilibrium Dislocation Distributions. *Acta Metallurgica et Materialia*, vol. 41, (no. 2), pp.625-642.

[81]**Wang, H. Y.; LeSar, R.** (1995): O(N) Algorithm for Dislocation Dynamics. *Philosophical Magazine A (Physics of Condensed Matter, Defects and Mechanical Properties)*, vol. 71, (no. 1), pp. 149-164.

[82]**Barts, D. B.; Carlsson, A. E.** (1995): Order-N Method for Force Calculation in Many-dislocation Systems. *Physical Review E (Statistical Physics, Plasmas, Fluids, and Related Interdisciplinary Topics)*, vol. 52, (no. 3, pt. B), pp. 3195-3204.

[83]**Raabe, D.** (1998): On the consideration of climb in discrete dislocation dynamics. *Philosophical Magazine A*, vol. 77, (no. 3), pp. 751.

[84]**deWit, R.** (1960): *Sol. State Phys.*, vol. 10, pp. 269.

[85]**Ghoniem, N. M.; Sun, L. Z.** (1999): Fast Sum Method for the Elastic Field of 3-D Dislocation Ensembles. *Physics Review B*, vol. 60, (no. 1), pp. 128-140.

[86]**Ghoniem, N. M.; Tong, S.-H.; Sun, L. Z.** (2000): Parametric Dislocation Dynamics: A Thermodynamics-based Approach to Investigations of Mesoscopic Plastic Deformation. *Physical Review B (Condensed Matter)*, vol. 61, (no. 2), pp.913-927.

[87]**Peach, M. O.; Koehler, J. S.** (1950): *Phys. Rev.*, vol. 80, pp. 436.

[88]**Ghoniem, N. M.; Huang, J.; Wang, Z.** (2001): Affine Covariant-contravariant Vector Forms for the Elastic Field of Parametric Dislocations in Isotropic Crystals. *Philosophical Magazine Letter*, in press.

[89]**Kubin, L. P.; Canova, G.; Condat, M.; Devincre, B.; Pontikis, V.; Brechet, Y.** (1992): Dislocation Microstructures and Plastic Flow: a 3D Simulation. *Diffusion and Defect Data - Solid State Data, Part B (Solid State Phenomena)*, vol. 23-24, pp.455-472.

[90]**Kubin, L. P.; Canova, G.** (1992): The Modelling of Dislocation Patterns. *Scripta Metallurgica et Materialia*, vol. 27, (no. 8), pp. 957-962.

[91]**Devincre, B.; Condat, M.** (1992): *Acta Metall. Mater.*, vol. 40, pp. 2629.

[92]**Canova, G.; Brechet, Y.; Kubin, L. P.** (1992): 3D dislocation simulation of plastic instabilities by work-softening in alloys. In *Modeling of Plastic Deformation and its Engineering Applications*, Eds. S. I. Anderson et al., RISØ National Laboratory, Roskilde, Denmark.

[93]**Kubin, L.P.** (1993): Dislocation Patterning During Multiple Slip of FCC Crystals. A Simulation Approach. *Physica Status Solidi A*, vol. 135, (no. 2), pp. 433-43

[94]**Canova, G. R.; Brecht, Y.; Kubin, L. P.; Devincre, B.; Pontikis, V.; Condat, M.** (1994): 3D Simulation of Dislocation Motion on a Lattice: Application to the Yield Surface of Single Crystals. *Diffusion and Defect Data Part B (Solid State Phenomena)*, vol. 35-36, pp. 101-106.

[95]**Devincre, B.; Kubin, L. P.** (1994): Simulations of Forest Interactions and Strain Hardening in FCC crystals. *Modelling and Simulation in Materials Science and Engineering*, vol. 2, (no. 3A), pp. 559-570.

[96]**Devincre, B.** (1996): Meso-scale Simulation of the Dislocation Dynamics, In *Computer Simulation in Materials Science*, Eds. H. 0. Krichner et al., Kluwer Academic Press, Dordrecht, pp. 309.

[97]**Devincre, B.; Kubin, L.** (1997): The Modelling of Dislocation Dynamics: Elastic Behaviour versus Core Properties. *Philosophical Transactions of the Royal Society London, Series A (Mathematical, Physical and Engineering Sciences), UK*, vol. 355(1731), pp. 2003.

[98]**Moulin, A.; Condat, M.; Kubin, L. P.** (1997): Simulation of Frank-Read Sources in Silicon. *Acta Materialia*, vol. 45, (no. 6), pp. 2339-2348.

[99]**Hirth, J. P.; Rhee, M.; Zbib, H.** (1996): Modeling of Deformation by a 3D Simulation of Multipole Curved Dislocations. *Journal of Computer-Aided Material. Design*, vol. 3, pp.164.

[100]**Zbib, H. M.; Rhee, M.; Hirth, J. P.** (1998): On Plastic Deformation and the Dynamics of 3D Dislocations. *International Journal of Mechanical Sciences*, vol. 40, (no. 2-3), pp.113-127.

[101]**Yoffe, E.H.** (1960): *Philosophical Magazine*, vol. 5, pp. 161.

[102]**Schwarz, K. V.; Tersoff, J.** (1996): Interaction of Threading and Misfit Dislocations in a Strained Epitaxial Layer. *Applied Physics Letters*, vol. 69, (no. 9), pp.1220-1222.

[103]**Schwarz, K. W.** (1997): Interaction of Dislocations on Crossed Glide Planes in a Strained Epitaxial Layer. *Physical Review Letters*, vol. 78, (no. 25), pp. 4785-4788.

[104]**Schwarz, K. W.; LeGoues, F. K.** (1997): Dislocation Patterns in Strained layers from Sources on Parallel Glide Planes. *Physical Review Letters*, vol. 79, (no. 10), pp. 1877-1880.

[105]**Brown, L. M.** (1967): *Philosophical Magazine*, vol. 15, pp. 363.

[106]**Ghoniem, N. M.** (1999): Curved Parametric Segments for the Stress Field of 3-D Dislocation Loops. *Transactions of the ASME. Journal of Engineering Materials and Technology*, vol. 121, (no. 2), pp. 136-142

[107]**Kukta, R. V.; Freund, L. B.** (1998): Three-dimensional Numerical Simulation of Interacting Dislocations in a Strained Epitaxial Surface Layer. in *M*ultiscale modelling of material, MRS Proceedings, edited by V.V. Bulatov, Tomas Diaz de la Rubia, R. Phillips, E. Kaxiras, and N. Ghoniem (Boston, Massachusetts, USA.

[108]**Khachaturyan, A. G.** (2000): in *T*he Science of Alloys for the 21st Century: A Hume-Rothery Symposium Celebration, Proceedings of a symposium of TMS, edited by E.A. Turchi, R.D. Shull and A. Gonis. TMS, 2000, pp. 293.

[109]**Wang, Y. U.; Jin, Y. M.; Cuitino, A. M.; Khachaturyan, A. G.** (2000): presented at the international conference *D*islocations 2000, the National Institute of Standards ans Technology, Gaithersburg, Jun3 19-22, 2000.

[110]**Wang, Y.U.; Jin, Y.M.; Cuitino, A. M.; Khachaturyan, A. G.** (2001): Nanoscale Phase Field Microelasticity Theory of Dislocations: Model and 3D Simulations. *Acta Materialia*, vol. 49, pp. 1847-1857.

[111]**Ghoniem, N. M.; Matthews, J. R.; Amodeo, R. J.** (1990): A Dislocation Model for Creep in Engineering Materials. *Res Mechanica*, vol. 29, (no. 3), pp. 197-219.

[112]**Gregor V. and Kratochvil J.** (1998): Self-organization approach to cyclic microplasticity; a model of a persistent slip band. *I*nternational Journal of Plasticity, vol. 14, pp. 159.

[113]**Neumann, P.** (1971): *Acta Metallurgica*, vol. 19, pp. 1233.

[114]**Essman, U.; Mughrabi, H.** *Philosophical Magazine*, vol. 40, pp. 731.

[115]**Kratochvil J.; Saxloà, N.** (1992): *Acta Metallurgica et Materialia*, vol. 26, pp. 113.

[116]**Saxloà, N.; Kratochvil, J.; Zatloukal, J.** (1997): The Model of Formation and Disintegration of Vein Dislocation Structure.*Materials Science & Engineering A*, vol. 234-236, pp. 205-208.

[117]**Kubin L. P.; Kratochvil, J.** (2000): Elastic model for the sweeping of dipolar loops. *Philosophical Magazine A*, vol. 80, pp. 201-218.

[118]**Wei, C.; Srivastav, D.; and Cho, K.**: Molecular Dynamics Study of Temperature Dependent Plastic Collapse of Carbon Nanotubes under Axial Compression. *CMES: Computer Modeling in Engineering & Sciences*, Vol. 3, No. 2, pp. 255-262.

[119]**Li,J. and Yip, S.**: Atomistic Measures of Materials Strength. *CMES: Computer Modeling in Engineering & Sciences*, Vol. 3, No. 2, pp. 219-228.

[120]**Liu, W. C.; Shi, S. Q.; Woo, C. H.; and Huang, H.**: Dislocation Nucleation and Propagation During Thin Film Deposition Under Tension. *CMES: Computer Modeling in Engineering & Sciences*, Vol. 3, No. 2, pp. 213-218.

[121]**Lin, K; and Chrzan, D. C.** : The Core Structure and Energy of the 90° Partial Dislocation in Si, *CMES: Computer Modeling in Engineering & Sciences*, Vol. 3, No. 2, pp. 201-212.

[122]**Kuramoto, E.; Ohsawa, K.; and Tsutsumi, T.** : Computer Simulation of Fundamental Behaviors of Point Defects, Clusters and Interaction with Dislocations in Fe and Ni. *CMES: Computer Modeling in Engineering & Sciences*, Vol. 3, No. 2, pp. 193-200.

[123]**Martinez R.; Ghoniem, N. M.**: The Influence of Crystal Surfaces on Dislocation Deformation: A Combined Dislocation Dynamics- Finite Element Approach. *CMES: Computer Modeling in Engineering & Sciences*, Vol. 3, No. 2, pp. 229-244.

[124]**Hsiung, L. M.; Lassila, D. H.** : Initial Dislocation Structure and Dynamic Dislocation Multiplication in Mo single Crystals. *CMES: Computer Modeling in Engineering & Sciences*, Vol. 3, No. 2, pp. 185-192.

[125]**Zhang, P.; Klein, P.; Huang, Y.; Gao, H.; and Wu, P. D.** : Numerical Simulation of Cohesive Fracture by the Virtual-Internal-Bond Model. *CMES: Computer Modeling in Engineering & Sciences*, Vol. 3, No. 2, pp. 263-278.

[126]**Garikipati, K.**: A Variational Multiscale Method to Embed Micromechanical Surface Laws in the Macromechanical Continuum Formulation. *CMES: Computer Modeling in Engineering & Sciences*, Vol. 3, No. 2, pp. 175-184.